

Coherent versus measurement feedback: Linear systems theory for quantum information

Naoki Yamamoto*

Department of Applied Physics and Physico-Informatics,
Keio University, Hiyoshi 3-14-1, Kohoku, Yokohama 223-8522, Japan
(Dated: October 13, 2014)

To control a quantum system via feedback, we generally have two options in choosing control scheme. One is the coherent feedback, which feeds the output field of the system, through a fully quantum device, back to manipulate the system without involving any measurement process. The other one is the measurement-based feedback, which measures the output field and performs a real-time manipulation on the system based on the measurement results. Both schemes have advantages/disadvantages, depending on the system and the control goal, hence their comparison in several situation is important. This paper considers a general open linear quantum system with the following specific control goals; back-action evasion (BAE), generation of a quantum non-demolished (QND) variable, and generation of a decoherence-free subsystem (DFS), all of which have important roles in quantum information science. Then some no-go theorems are proven, clarifying that those goals cannot be achieved by any measurement-based feedback control. On the other hand it is shown that, for each control goal, there exists a coherent feedback controller accomplishing the task. The key idea to obtain all the results is system theoretic characterizations of BAE, QND, and DFS in terms of controllability and observability properties or transfer functions of linear systems, which are consistent with their standard definitions.

I. INTRODUCTION

Should we perform measurement or not? This question appears to be critical in quantum physics, particularly in quantum information science. For quantum computation, for instance, it is of essential importance to study differences between the conventional closed-system approach and the measurement-based one (i.e. the so-called one-way computation). This paper focuses on a specific aspect of this abstract and broad question; we will consider feedback control problems. That is, for a given open system (plant), we want to engineer another system (controller) connected to the plant so that the plant or the whole system behaves in a desirable way. The fundamental question is then, in our case, as follows; *should we measure the plant or not, for engineering a closed-loop system?* More precisely, in the former case, we measure the plant's output and engineer a classical controller that manipulates the plant using the measurement result – this is called the *measurement-based feedback (MF)* approach. In the latter case, we do not measure it, but rather connect a fully quantum controller directly to the plant system in a feedback manner – this is called the *coherent feedback (CF)* approach.

A typical example is shown in Fig. 1; the plant is an open mechanical oscillator coupled to a ring-type optical cavity, and the control goal is to minimize the energy of the oscillator, or equivalently to cool the oscillator towards its motional ground state. As mentioned above, there are two feedback control strategies. One is the MF controller (Fig. 1 (a)) that measures the output

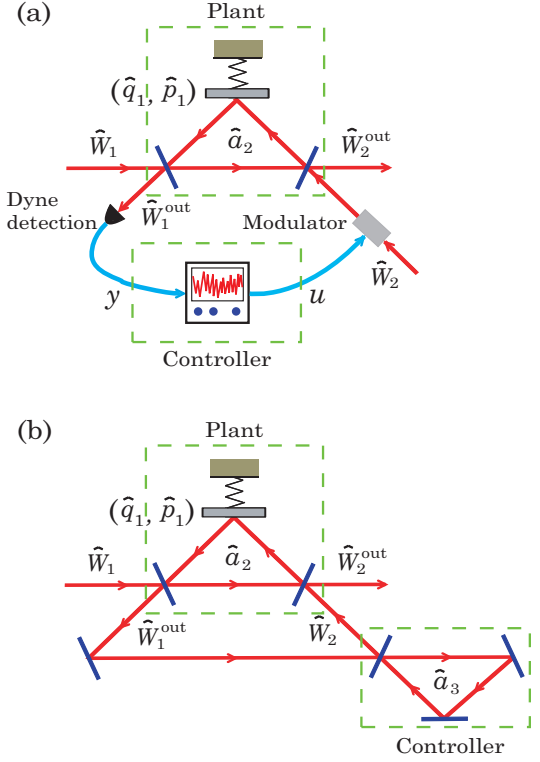


FIG. 1: Example of (a) measurement-based feedback and (b) coherent feedback, for cooling a mechanical oscillator.

field \hat{W}_1^{out} by for instance a homodyne detector; then, using the continuous-time measurement results $y(t)$, it produces the control signal $u(t)$ for modulating the input field \hat{W}_2 . The other option is the CF control (Fig. 1 (b)), where we construct another fully quantum system that

*yamamoto@appi.keio.ac.jp

feeds the output field \hat{W}_1^{out} back to the input field \hat{W}_2 , without involving any measurement component. The question is then about how to design a MF/CF controller that cools the oscillator most effectively.

Controller synthesis for a quantum system is in general non-trivial, but researchers' longstanding efforts have built a solid mathematical framework for dealing with those problems. For the MF case, actually there exists a beautiful *quantum feedback control theory* [1, 2, 3] that was developed based on the *quantum filtering* [4, 5, 6] together with the classical control theory [7, 8, 9]. In fact, the above-described cooling problem can be formulated as a quantum Linear Quadratic Gaussian (LQG) feedback control problem and explicitly solved [1, 10, 11, 12, 13]. Also the theory has been applied to various control problems in quantum information science such as error correction [14, 15, 16]. Notably, experiment of MF control is now within the reach of current technologies [17, 18, 19, 20]. The CF control, on the other hand, has still a relatively young history though its initial concept was found in [21] back in 1994; but recently it has attracted increasing attention, leading as a result development of the basic control theory [22, 23, 24, 25] and applications [26, 27, 28, 29]. Some experimental demonstrations of CF control [30, 31, 32, 33] also warrant special mention; in fact, one of the main advantages of CF is in its experimental feasibility compared to the MF approach.

Let us return to our question; which controller, MF or CF, is better? Now note that a CF controller is a fully quantum system whose random variables are in general represented by non-commutative operators, while a MF controller is a classical system with commutative random variables. Hence from a mathematical viewpoint the class of MF controllers is completely included in that of CF controllers. Thus our question is as follows; *in what situation is a CF controller better than a MF controller?* Actually there have been several studies exploring answers to this question [12, 13, 21, 34, 35]; most of these studies discussed problems of minimizing a certain cost function such as energy of an oscillator or the time required for state transfer. In particular in [12, 13], the authors studied the problem discussed in the second paragraph and clarified that a certain CF controller outperforms any MF controller when the total mean phonon number of the oscillator is in the quantum regime; in other words, the two types of controllers do not show a clear difference in their performance for cooling, in a classical situation. This in more broad sense implies that a CF controller would outperform a MF controller only in a purely quantum regime. Consequently, our question can be regarded as a special case of the fundamental problem in physics asking in what situation a fully quantum device (such as a quantum computer) outperforms any classical one (such as a classical computer).

Towards shedding a new light on the above-mentioned fundamental problem, this paper attempts to clarify a boundary between the CF and MF controls for specific

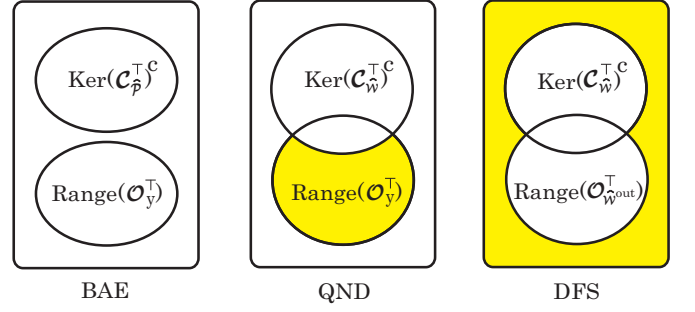


FIG. 2: Systematic characterizations of BAE, QND, and DFS, represented by the set of vectors $v \in \mathbb{R}^{2n}$, where the corresponding quantum variables are given by $v^\top \hat{x}$. $\text{Ker}(\mathcal{C}_\bullet^\top)^c$ and $\text{Range}(\mathcal{O}_\bullet^\top)$ denote the controllable and observable subspaces, respectively. The colored region represents the set of QND variables (middle) and the set of variables in a DFS (right).

control problems. The problems are not what aim to minimize a cost function, but we will consider the following three; (i) realization of a back-action evasion (BAE) measurement, (ii) generation of a quantum non-demolished (QND) variable, and (iii) generation of a decoherence-free subsystem (DFS). The followings are brief descriptions of these notions in the input-output formalism [36, 37]. First, if a measurement process is subjected only to a single noise quadrature (shot noise) and not to its conjugate (back-action noise), then it is called the BAE measurement [38, 39]; as a result BAE may beat the so-called standard quantum limit (SQL) and enables high-precision detection for a tiny signal such as a gravitational wave force. Next, a QND variable is a physical quantity that can be measured without being disturbed [40]; more precisely, it is not affected by an input probe field but still appears in the output field, which can be thus measured repeatedly. Lastly, a DFS is a subsystem that is completely isolated from surrounding environment; that is, it is a subsystem whose variables are not affected by any input probe/environment field, and further, they do not appear in the corresponding output fields. Hence, a DFS can be used for quantum computation or memory [41, 42]. These three notions play crucial roles especially in quantum information science, thus their realizations are of essential importance. Indeed we find in the literature some feedback-based approaches realizing BAE [43, 44, 45], QND [46], and DFS [47, 48, 49].

Another feature of this paper is that we focus on general open *linear quantum systems* [1, 36, 37]; this is a wide class of systems containing for instance optical devices [50], mechanical oscillators [12, 13, 43, 44, 45, 51, 52, 53, 54, 55, 56, 57], and large atomic ensembles [58, 59, 60, 61, 62]. Linear systems are typical continuous-variables (CV) systems [63, 64], which are applicable to several CV quantum information processing both in Gaussian case [65, 66] and non-Gaussian case [67, 68, 69]. In both classical and quantum cases, for linear systems, the so-called *controllability* and *ob-*

TABLE I: The no-go theorems (left column). For both “types” of control configurations, any MF controller cannot achieve the control goals; i.e. realization of BAE measurement, generation of a QND variable, and generation of a DFS. On the other hand, in every category we can find a CF controller achieving the task (right column).

(type 1)	MF	CF
BAE	⊘	✓
QND	⊘	✓
DFS	⊘	✓
(type 2)	MF	CF
BAE	⊘	✓
QND	⊘	✓
DFS	⊘	✓

servability properties can be well defined; further, those properties have equivalent representations in terms of a *transfer function*, which explicitly describes the relation between input and output. In fact a main advantage of focusing on linear systems is that we can have systematic characterizations of BAE, QND, and DFS in terms of the controllability and observability properties or transfer functions, which are consistent with the standard definitions found in the literature. Figure 2 is an at a glance overview of those characterizations, showing unification of the notions. Indeed this is the key idea to obtain all the results in this paper.

Therefore our problem is, for a given open linear system, to design a CF/MF controller to realize BAE, QND, or DFS. For this problem, the results summarized in Table I are obtained. That is, no MF controller can achieve any of the control goals for general linear systems (there are two kinds of general configurations for feedback control, as indicated by “type” in Table I). In contrast to these no-go theorems, for every category in the table we can find an example of CF controller achieving the goal. From the viewpoint of the above-mentioned fundamental question asking differences of the ability of quantum and classical devices, therefore, these results imply that BAE, QND, and DFS are the properties that can only be realized in a fully quantum device.

This paper is organized as follows. Section II reviews some useful facts in classical linear systems theory and describes a general linear quantum system with some examples. In Sec. III we discuss the three control goals, BAE, QND, and DFS, in the general input-output formalism and give their systematic characterizations in terms of the controllability-observability properties and also transfer functions; again, these new characterizations are special feature of this paper. Then the proofs of the no-go theorems are given in Secs. IV and V, each of which are devoted to the proofs for the type-1 and the type-2 MF control configuration, respectively. Sections

VI and VII demonstrate systematic engineering of a CF controller achieving the control goal. In particular, in the type-2 case, we will study a Michelson’s interferometer composed of two mechanical oscillators, which is used for gravitational wave detection.

Notations: For a matrix A , the *kernel* and the *range* are defined by $\text{Ker}(A) = \{x | Ax = 0\}$ and $\text{Range}(A) = \{y | y = Ax, \forall x\}$, respectively. The complement of a linear space \mathcal{X} is denoted by \mathcal{X}^c . \emptyset means the null space. In this paper we do not use the terminology “observable” to represent a measurable physical quantity (i.e. a self adjoint operator), because it has a different meaning in systems theory; a physical quantity is called a “variable”, e.g. a QND variable rather than a QND observable.

II. PRELIMINARIES: LINEAR SYSTEMS THEORY AND LINEAR QUANTUM SYSTEMS

A. Linear systems theory

A standard form of classical linear systems is given by

$$\frac{dx}{dt} = Ax + Bu, \quad y = Cx. \quad (1)$$

$x(t) \in \mathbb{R}^n$ is a vector of n c-number variables. $u(t)$ and $y(t)$ are vectors of real-valued input and output signals, respectively. A, B , and C are real matrices with appropriate dimensions. In this paper, the following three questions are important; (i) which components of x can be controlled by u , (ii) which components of x can be observed from y , and (iii) in what condition u does not appear in y ? The answers are briefly described below. See [7, 8, 9] for more detailed discussion.

The first problem can be explicitly solved by examining the following *controllability matrix*:

$$\mathcal{C}_u = [B, AB, A^2B, \dots, A^{n-1}B]. \quad (2)$$

Indeed this matrix fully characterizes the controllable and uncontrollable variables with respect to (w.r.t.) $u(t)$. To see this fact, suppose $m = \dim \text{Range}(\mathcal{C}_u) < n$ and let $\{d_i^{(1)}\}$ and $\{d_i^{(2)}\}$ be independent vectors spanning $\text{Range}(\mathcal{C}_u)$ and $\text{Range}(\mathcal{C}_u)^c$, respectively. Further let us define $T_1 = [d_1^{(1)}, \dots, d_m^{(1)}]$ and $T_2 = [d_1^{(2)}, \dots, d_{n-m}^{(2)}]$. Then, as $A\mathcal{C}_u$ is spanned by $\{d_i^{(1)}\}$, there exists a matrix A_{11} satisfying $AT_1 = T_1A_{11}$. On the other hand AT_2 is in general spanned by all the vectors; i.e. $AT_2 = T_1A_{12} + T_2A_{22}$. Note also that there exists a matrix B_1 satisfying $B = T_1B_1$. These relations are summarized in terms of the invertible square matrix $T = [T_1, T_2]$ as

$$AT = T \begin{bmatrix} A_{11} & A_{12} \\ 0 & A_{22} \end{bmatrix}, \quad B = T \begin{bmatrix} B_1 \\ 0 \end{bmatrix}.$$

Thus the dynamics of $x' = T^{-1}x$ is given by

$$\frac{dx'}{dt} = \begin{bmatrix} A_{11} & A_{12} \\ 0 & A_{22} \end{bmatrix} x' + \begin{bmatrix} B_1 \\ 0 \end{bmatrix} u. \quad (3)$$

Clearly $x'_2 = V_2^\top x$ is free from u , where $[V_1, V_2]^\top = T^{-1}$; in particular, due to $V_2^\top T_1 = 0$, the uncontrollable variable x'_2 is characterized by $\text{Range}(V_2) = \text{Ker}(\mathcal{C}_u^\top)$. Also the controllable one $x'_1 = V_1^\top x$ is defined in $\text{Range}(V_1) = \text{Ker}(\mathcal{C}_u^\top)^c$. Hence we call these sets the *uncontrollable subspace* and the *controllable subspace*, respectively [82]. The following fact is especially useful in this paper: the system has an uncontrollable variable $r = v^\top x$ iff

$$v \in \text{Ker}(\mathcal{C}_u^\top) \Leftrightarrow v^\top A^k B = 0, \quad \forall k \geq 0. \quad (4)$$

The answer to the second question is obtained in a similar fashion. Let us define the *observability matrix*

$$\mathcal{O}_y = [C^\top, A^\top C^\top, (A^2)^\top C^\top, \dots, (A^{n-1})^\top C^\top]^\top. \quad (5)$$

Assume $\dim \text{Ker}(\mathcal{O}_y) = \ell < n$. Then, there exists a linear transformation $x \rightarrow x' = [x'_1{}^\top, x'_2{}^\top]^\top$ with $x'_2 \in \mathbb{R}^\ell$ such that the system equations are of the following form:

$$\frac{dx'}{dt} = \begin{bmatrix} A_{11} & 0 \\ A_{21} & A_{22} \end{bmatrix} x' + \begin{bmatrix} B_1 \\ B_2 \end{bmatrix} u, \quad y = [C_1, 0]x'. \quad (6)$$

Thus x'_1 and x'_2 constitute the observable and unobservable subsystems w.r.t. y , respectively. The variables are represented by $x'_1 = U_1^\top x$ with $\text{Range}(U_1) = \text{Range}(\mathcal{O}_y^\top)$ and $x'_2 = U_2^\top x$ with $\text{Range}(U_2) = \text{Range}(\mathcal{O}_y^\top)^c$; as in the above case, we call these subspaces the *observable subspace* and *unobservable subspace*, respectively. In particular, there always exists a coordinate transformation such that $r = v^\top x$ is unobservable if and only if

$$v \in \text{Ker}(\mathcal{O}_y) \Leftrightarrow C A^k v = 0, \quad \forall k \geq 0. \quad (7)$$

The above two facts readily leads to the answer to the third question; that is, there is no subsystem that is controllable w.r.t. u and observable w.r.t. y , which is algebraically represented by

$$\text{Ker}(\mathcal{C}_u^\top)^c \cap \text{Range}(\mathcal{O}_y^\top) = \emptyset \Leftrightarrow C A^k B = 0, \quad \forall k \geq 0. \quad (8)$$

Note that this is further equivalent to $\text{Range}(\mathcal{C}_u) \subseteq \text{Ker}(\mathcal{O}_y)$, which particularly implies $C T_1 = 0$ with T_1 defined below Eq. (2). Hence we have

$$y = Cx = CTT^{-1}x = C[T_1, T_2]x' = [0, CT_2]x',$$

where $x' = T^{-1}x$. Together with Eq. (3), we now see that u acts only on $x'_1 = V_1^\top x$ while x'_1 is not visible from y ; accordingly, u does not appear in y .

The above conditions (4), (7), and (8) can be represented in terms of a *transfer function*; let us define the Laplace transformation of a time-varying signal $z(t)$ by

$$z[s] := \int_0^\infty z(t)e^{-st}dt, \quad \text{Re}(s) > 0.$$

In the Laplace domain, Eq. (1) is represented by $sx[s] = Ax[s] + Bu[s]$ and $y[s] = Cx[s]$, which consequently yield

$$y[s] = \Xi_{u \rightarrow y}[s]u[s], \quad \Xi_{u \rightarrow y}[s] = C(sI - A)^{-1}B.$$

Thus, the signal flow from u to y is explicitly characterized by the transfer function $\Xi_{u \rightarrow y}[s]$. We then readily see from the polynomial expansion of $\Xi_{u \rightarrow y}[s]$ w.r.t. s that the condition (8) is equivalent to

$$\Xi_{u \rightarrow y}[s] = 0, \quad \forall s. \quad (9)$$

Likewise, Eqs. (4) and (7) are respectively equivalent to

$$\Xi_{u \rightarrow x'_2}[s] = 0, \quad \forall s \quad \text{and} \quad \Xi_{x'_2 \rightarrow y}[s] = 0, \quad \forall s. \quad (10)$$

B. Linear quantum systems

In this paper, we consider a general open system composed of n oscillators with canonical conjugate pairs \hat{q}_i and \hat{p}_i ($i = 1, \dots, n$). Let us collect them into a single vector as $\hat{x} = [\hat{q}_1, \hat{p}_1, \dots, \hat{q}_n, \hat{p}_n]^\top$. Then, the CCR $\hat{q}_i \hat{p}_j - \hat{p}_j \hat{q}_i = i\delta_{ij}$ (we assume $\hbar = 1$) is represented by

$$\begin{aligned} \hat{x} \hat{x}^\top - (\hat{x} \hat{x}^\top)^\top &= i\Sigma_n, \\ \Sigma_n &= \text{diag}\{\sigma, \dots, \sigma\}, \quad \sigma = \begin{bmatrix} 0 & 1 \\ -1 & 0 \end{bmatrix}. \end{aligned} \quad (11)$$

Σ_n is a $2n \times 2n$ block diagonal matrix; we often omit the subscript n . The system is driven by the Hamiltonian

$$\hat{H} = \hat{x}^\top G \hat{x} / 2,$$

where $G = G^\top \in \mathbb{R}^{2n \times 2n}$. Further, it couples to environment/probe fields through the Hamiltonian $\hat{H}_{\text{int}} = i \sum_j (\hat{L}_j \hat{A}_j^* - \hat{L}_j^* \hat{A}_j)$, where $\hat{L}_j = c_j^\top \hat{x}$ ($c_j \in \mathbb{C}^{2n}$, $j = 1, \dots, m$). Also \hat{A}_j is the annihilation operator on the j th field, which under the Markovian approximation satisfies $[\hat{A}_i(t), \hat{A}_j^*(t')] = \delta_{ij} \delta(t - t')$; i.e. it is the white noise operator. Then, the Heisenberg equations of \hat{q}_j and \hat{p}_j are summarized to the following linear equation [1, 36, 37]:

$$\frac{d\hat{x}}{dt} = A\hat{x} + \Sigma_n C^\top \Sigma_m \dot{\mathcal{W}}. \quad (12)$$

The coefficient matrices are given by $A = \Sigma_n(G + C^\top \Sigma_m C / 2) \in \mathbb{R}^{2n \times 2n}$ (the second term is the Ito-correction term) and

$$C = \sqrt{2}[\Re(c_1), \Im(c_1), \dots, \Re(c_m), \Im(c_m)]^\top \in \mathbb{R}^{2m \times 2n}.$$

Also we have defined $\hat{\mathcal{W}} = [\hat{Q}_1, \hat{P}_1, \dots, \hat{Q}_m, \hat{P}_m]^\top$, where

$$\hat{Q}_j = (\hat{A}_j + \hat{A}_j^*)/\sqrt{2}, \quad \hat{P}_j = (\hat{A}_j - \hat{A}_j^*)/\sqrt{2}i. \quad (13)$$

Further, the field variables change to

$$\hat{\mathcal{W}}^{\text{out}} = C\hat{x} + \hat{\mathcal{W}}. \quad (14)$$

The set of equations (12) and (14) is the most general form of open *linear quantum systems*.

All the $2m$ elements of the vector $\hat{\mathcal{W}}^{\text{out}}$ in Eq. (14) cannot be measured simultaneously, because they do not

commute with each other. In fact, without introducing additional noise fields as explained just later, we can measure only at most half of them; that is, the output equation associated with a *linear measurement*, which is realized by a Homodyne detector, is of the form

$$y = M_1 \hat{\mathcal{W}}^{\text{out}} = M_1 C \hat{x} + M_1 \hat{\mathcal{W}}, \quad (15)$$

where M_1 is a $m \times 2m$ real matrix satisfying $M_1 \Sigma_m M_1^\top = 0$ and $M_1 M_1^\top = I$. Actually, all the elements of $y(t)$ are classical signals commuting with each other as well as with those of $y(t')$ for all times t, t' ; i.e.

$$[y_i(t), y_j(t')] = 0, \quad \forall i, j, \quad \forall t, t'.$$

Let us further introduce $\bar{y} = M_2 \hat{\mathcal{W}}^{\text{out}}$ with matrix M_2 such that $M^\top = [M_1^\top, M_2^\top]$ is a symplectic and orthogonal matrix, which as a result leads to

$$\begin{aligned} M_2 \Sigma_m M_2^\top &= 0, \quad M_2 M_2^\top = I, \quad M_1 \Sigma_m M_2^\top = I, \\ M_1 M_2^\top &= 0, \quad M_1^\top M_1 + M_2^\top M_2 = I. \end{aligned} \quad (16)$$

The elements of \bar{y} correspond to the canonical conjugate operators to those of Eq. (15); i.e. the CCR $y(t)\bar{y}^\top(t') - (\bar{y}(t')y^\top(t))^\top = i\delta(t-t')I$ holds.

If we want to measure all the quadratures of $\hat{\mathcal{W}}^{\text{out}}$, it is still possible by introducing additional noise fields $\hat{\mathcal{V}} = [\hat{Q}'_1, \hat{P}'_1, \dots, \hat{Q}'_m, \hat{P}'_m]^\top$ and performing Homodyne measurement on the joint fields composed of $\hat{\mathcal{W}}^{\text{out}}$ and $\hat{\mathcal{V}}$; that is, the output equation is given by

$$y = M_1 \begin{bmatrix} \hat{\mathcal{W}}^{\text{out}} \\ \hat{\mathcal{V}} \end{bmatrix} = M_1 \begin{bmatrix} C \\ 0 \end{bmatrix} \hat{x} + M_1 \begin{bmatrix} \hat{\mathcal{W}} \\ \hat{\mathcal{V}} \end{bmatrix}, \quad (17)$$

where in this case M_1 is with the size $2m \times 4m$ and it satisfies $M_1 \Sigma_{2m} M_1^\top = 0$, etc. We thus have $2m$ measurement outcomes, though they are subjected to the additional noise. Note that, by simply replacing C and $\hat{\mathcal{W}}$ by $[C^\top, 0]^\top$ and $[\hat{\mathcal{W}}^\top, \hat{\mathcal{V}}^\top]^\top$, this dual Homodyne detection scheme can be represented by Eqs. (12) and (15). Hence in what follows, without loss of generality, we use Eq. (15) to represent the most general linear measurement.

C. Examples

(i) A simple open linear system is an empty optical cavity with two input and output fields, depicted in Fig. 3 (a). The system equations are given by

$$\begin{aligned} \frac{d\hat{a}}{dt} &= -(\kappa_1 + \kappa_2)\hat{a} - \sqrt{2\kappa_1}\hat{A}_1 - \sqrt{2\kappa_2}\hat{A}_2, \\ \hat{A}_1^{\text{out}} &= \sqrt{2\kappa_1}\hat{a} + \hat{A}_1, \quad \hat{A}_2^{\text{out}} = \sqrt{2\kappa_2}\hat{a} + \hat{A}_2. \end{aligned}$$

\hat{a} is the annihilation operator of the cavity mode. \hat{A}_j and \hat{A}_j^{out} are the white noise operators of the j th incoming and the outgoing optical fields, respectively. κ_j is the coupling strength between \hat{a} and the j th field, which is

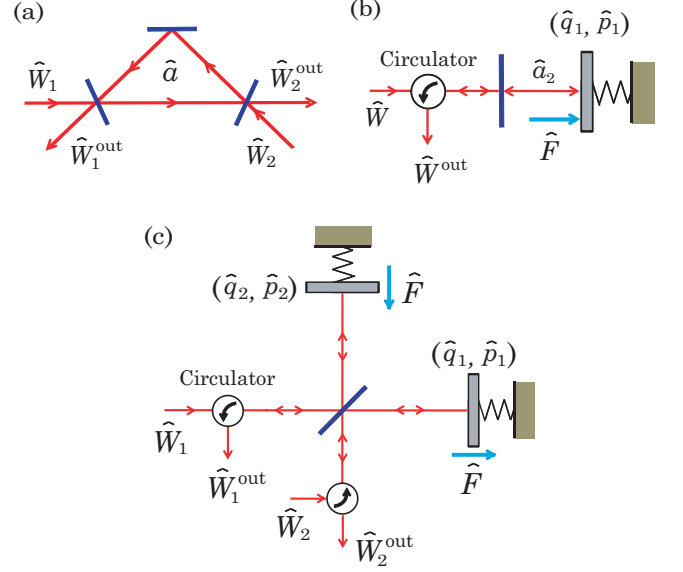


FIG. 3: Examples of open linear quantum systems. (a) Optical cavity with two input and output fields, (b) Mechanical oscillator coupled to an optical cavity, and (c) Michelson's interferometer with two identical oscillators.

proportional to the transmissivity of the coupling mirror. In this paper we express the variables in the quadrature form, which in this case are defined as $\hat{x} = [\hat{q}, \hat{p}]^\top$ with $\hat{q} = (\hat{a} + \hat{a}^*)/\sqrt{2}$ and $\hat{p} = (\hat{a} - \hat{a}^*)/\sqrt{2}i$. Also $\hat{W}_j = [\hat{Q}_j, \hat{P}_j]^\top$ with the field quadratures (13). Then, the above system equations are rewritten as

$$\begin{aligned} \frac{d\hat{x}}{dt} &= -(\kappa_1 + \kappa_2)\hat{x} - \sqrt{2\kappa_1}\hat{W}_1 - \sqrt{2\kappa_2}\hat{W}_2, \\ \hat{W}_1^{\text{out}} &= \sqrt{2\kappa_1}\hat{x} + \hat{W}_1, \quad \hat{W}_2^{\text{out}} = \sqrt{2\kappa_2}\hat{x} + \hat{W}_2. \end{aligned}$$

Typically this system works as a low-pass filter [50]; that is, for the noisy input field \hat{W}_1 , the corresponding mode-cleaned output field \hat{W}_2^{out} is generated, which will be used later for e.g. some quantum information processing. To attain this goal, \hat{W}_1^{out} is measured to detect the error signal for locking the optical path length in the cavity. Note that \hat{W}_2 is a vacuum field. That is, in this case, the two input-output fields have different roles.

(ii) The mechanical oscillator shown in Fig. 3 (b) can also be modeled as a linear system. This system is composed of a mechanical oscillator with mode (\hat{q}_1, \hat{p}_1) and a cavity with mode $\hat{a}_2 = (\hat{q}_2 + i\hat{p}_2)/\sqrt{2}$. The cavity couples to a probe field $\hat{W} = [\hat{Q}, \hat{P}]^\top$. After linearization, the system equation of $\hat{x} = [\hat{q}_1, \hat{p}_1, \hat{q}_2, \hat{p}_2]^\top$ is obtained as

$$\begin{aligned} \frac{d\hat{x}}{dt} &= \begin{bmatrix} 0 & 1/m & 0 & 0 \\ -m\omega^2 & 0 & \kappa & 0 \\ 0 & 0 & -\gamma & 0 \\ \kappa & 0 & 0 & -\gamma \end{bmatrix} \hat{x} - \sqrt{2\gamma} \begin{bmatrix} 0 & 0 \\ 0 & 0 \\ 1 & 0 \\ 0 & 1 \end{bmatrix} \hat{W}, \\ \hat{W}^{\text{out}} &= \sqrt{2\gamma} \begin{bmatrix} 0 & 0 & 1 & 0 \\ 0 & 0 & 0 & 1 \end{bmatrix} \hat{x} + \hat{W}. \end{aligned}$$

m and ω are the mass and the resonant frequency of the oscillator. κ is the coupling constant between the oscillator and the cavity field, which is proportional to the strength of radiation pressure force. γ is the coupling constant between the cavity and the probe field. As indicated from the equations, it is possible to extract some information about the oscillator's behavior by measuring the probe output field \hat{W}^{out} . A typical situation is that the oscillator is pushed by an external force \hat{F} with unknown strength; we attempt to estimate this value, by measuring \hat{W}^{out} . The oscillator's motion is usually much slower than that of the cavity field, thus we can adiabatically eliminate the cavity mode and have a reduced dynamical equation of only the oscillator:

$$\begin{aligned} \frac{d\hat{x}}{dt} &= \begin{bmatrix} 0 & 1/m \\ -m\omega^2 & 0 \end{bmatrix} \hat{x} + \sqrt{\lambda} \begin{bmatrix} 0 \\ 1 \end{bmatrix} \hat{Q} + \begin{bmatrix} 0 \\ 1 \end{bmatrix} \hat{F}, \\ \hat{W}^{\text{out}} &= \begin{bmatrix} \hat{Q}^{\text{out}} \\ \hat{P}^{\text{out}} \end{bmatrix} = \sqrt{\lambda} \begin{bmatrix} 0 & 0 \\ 1 & 0 \end{bmatrix} \hat{x} + \begin{bmatrix} \hat{Q} \\ \hat{P} \end{bmatrix}, \end{aligned} \quad (18)$$

where $\lambda = 2\kappa^2/\gamma$ represents the strength of the direct coupling between the oscillator and the probe field. This equation clearly shows that only \hat{P}^{out} contains the information about the oscillator and accordingly \hat{F} ; thus \hat{P}^{out} should be measured, implying $M_1 = [0, 1]$ in Eq. (15).

(iii) The last example is the Michelson's interferometer composed of two identical mechanical oscillators with mass m and resonant frequency ω , depicted in Fig. 3 (c). This is a simplest configuration among various schemes that are expected to have capability of direct detection of a gravitational wave (GW) [38, 39, 56, 57]. A basic detection mechanism is as follows. A coherent light field \hat{W}_1 is injected into the left input port (bright port), while in the other port (dark port) the input \hat{W}_2 is set to be a vacuum. If a gravitational wave comes, one arm shrinks while the other one extends, thereby the oscillators experience tiny force along opposite directions, \hat{F} and $-\hat{F}$. As a result the dynamics of the two oscillators can be modeled by the combination of Eq. (18):

$$\begin{aligned} \frac{d\hat{x}}{dt} &= \begin{bmatrix} 0 & 1/m \\ -m\omega^2 & 0 \end{bmatrix} \hat{x} \\ &+ \begin{bmatrix} 0 \\ \sqrt{\lambda} \\ 0 \\ \sqrt{\lambda} \end{bmatrix} \hat{Q}_1 + \begin{bmatrix} 0 \\ \sqrt{\lambda} \\ 0 \\ -\sqrt{\lambda} \end{bmatrix} \hat{Q}_2 + \begin{bmatrix} 0 \\ 1 \\ 0 \\ -1 \end{bmatrix} \hat{F}, \\ \begin{bmatrix} \hat{W}_1^{\text{out}} \\ \hat{W}_2^{\text{out}} \end{bmatrix} &= \sqrt{\lambda} \begin{bmatrix} 0 & 0 \\ 1 & 0 \\ 0 & 0 \\ 1 & -1 \end{bmatrix} \hat{x} + \begin{bmatrix} \hat{W}_1 \\ \hat{W}_2 \end{bmatrix}. \end{aligned} \quad (19)$$

Let us rewrite this equation in terms of the common modes $\hat{q}'_1 = (\hat{q}_1 + \hat{q}_2)/\sqrt{2}$, $\hat{p}'_1 = (\hat{p}_1 + \hat{p}_2)/\sqrt{2}$ and the differential modes $\hat{q}'_2 = (\hat{q}_1 - \hat{q}_2)/\sqrt{2}$, $\hat{p}'_2 = (\hat{p}_1 - \hat{p}_2)/\sqrt{2}$. Then these two modes are decoupled and the force \hat{F} appears only in the dynamics of $\hat{x}'_2 = [\hat{q}'_2, \hat{p}'_2]^\top$, which is

exactly the same as Eq. (18):

$$\begin{aligned} \frac{d\hat{x}'_2}{dt} &= \begin{bmatrix} 0 & 1/m \\ -m\omega^2 & 0 \end{bmatrix} \hat{x}'_2 + \sqrt{\lambda} \begin{bmatrix} 0 \\ 1 \end{bmatrix} \hat{Q}_2 + \begin{bmatrix} 0 \\ 1 \end{bmatrix} \hat{F}, \\ \hat{Q}_2^{\text{out}} &= \hat{Q}_2, \quad \hat{P}_2^{\text{out}} = \sqrt{\lambda} \hat{q}'_2 + \hat{P}_2. \end{aligned} \quad (20)$$

Thus, ideally, by measuring \hat{P}_2^{out} we can detect \hat{F} .

III. SYSTEM THEORETIC CHARACTERIZATION OF BAE, QND, DFS

The problem considered in this paper is to design a MF/CF controller connected to the plant system so that the plant or the whole closed-loop system achieves a certain control goal. We consider the following three goals: realization of back-action evasion (BAE) measurement, generation of a quantum non-demolished (QND) variable, and generation of a decoherence-free subsystem (DFS). Actually there are a lot of works investigating their mathematical characterizations, physical realizations, and applications especially in quantum information science. This section shows system theoretic characterizations of these notions in terms of controllability and observability properties or transfer functions, in a consistent way with the standard definitions.

A. BAE

The idea of BAE originally comes from the research for GW detection. The Michelson's interferometer described in Sec. II-C is a simplest system for this purpose, and we now know from Eq. (20) that the measurement output $y = \hat{P}_2^{\text{out}} = \sqrt{\lambda} \hat{q}'_2 + \hat{P}_2$ would offer some information about \hat{F} . The issue is that, in addition to the unavoidable noise \hat{P}_2 called the *shot noise*, the output y contains the conjugate \hat{Q}_2 , which is called the *back-action (BA) noise*, as seen explicitly in the Laplace domain:

$$y[s] = \frac{\sqrt{\lambda}}{m(s^2 + \omega^2)} (\sqrt{\lambda} \hat{Q}_2[s] + \sqrt{2} \hat{F}[s]) + \hat{P}_2[s].$$

The slight change of the oscillator's position due to the GW effect, \hat{g} , is defined in the Fourier domain $s = i\Omega$ as $\hat{F}[i\Omega] = -mL\Omega^2 \hat{g}[i\Omega]$, where L is the optical path length in the interferometer. Hence under the assumption $\Omega \gg \omega$, the normalized signal containing \hat{g} is given by

$$\tilde{y}[i\Omega] = \frac{y[i\Omega]}{2\sqrt{\lambda}L} = \hat{g}[i\Omega] + \frac{\sqrt{\lambda}}{mL\Omega^2} \hat{Q}_2[i\Omega] + \frac{1}{2\sqrt{\lambda}L} \hat{P}_2[i\Omega].$$

The noise power of \tilde{y} is bounded from below by the following *standard quantum limit (SQL)*:

$$\begin{aligned} S[i\Omega] &= \langle |\tilde{y} - \hat{g}|^2 \rangle = \frac{\lambda}{m^2 L^2 \Omega^4} \langle |\hat{Q}_2|^2 \rangle + \frac{1}{4\lambda L^2} \langle |\hat{P}_2|^2 \rangle \\ &\geq 2\sqrt{\frac{\langle |\hat{Q}_2|^2 \rangle \langle |\hat{P}_2|^2 \rangle}{4m^2 L^4 \Omega^4}} \geq \frac{1}{2mL^2 \Omega^2} = S_{\text{SQL}}[i\Omega]. \end{aligned} \quad (21)$$

The last inequality is due to the Heisenberg uncertainty relation $\langle |\hat{Q}_2|^2 \rangle \langle |\hat{P}_2|^2 \rangle \geq 1/4$. (For the simple notation, the power spectrum is defined without involving the delta function.) The SQL appears because the output y contains the BA noise \hat{Q}_2 in addition to the shot noise \hat{P}_2 . Thus, towards high-precision detection of \hat{g} , a special system configuration should be devised so that y is free from \hat{Q}_2 . That is, we need BAE. In fact, if BAE is realized, then by injecting a \hat{P}_2 -squeezed light field into the dark port, we can possibly reduce the noise power below the SQL and may have chance to detect \hat{g} ; for some specific configurations achieving BAE, see [38, 39, 52, 56, 57].

The above discussion can be generalized for the system (12) and (15). Let us assume that the signal to be detected is contained in the output (15):

$$y = M_1 \hat{W}^{\text{out}} = M_1 C \hat{x} + M_1 \hat{W} = M_1 C \hat{x} + \hat{Q}. \quad (22)$$

Hence, $\hat{Q} = M_1 \hat{W}$ is the shot noise, which must appear in y . The BA noise is then given by the conjugate $\hat{P} = M_2 \hat{W}$. Note that these are vectors of operators: $\hat{Q} = [\hat{Q}_1, \dots, \hat{Q}_m]^\top$ and $\hat{P} = [\hat{P}_1, \dots, \hat{P}_m]^\top$. The matrices M_1 and M_2 satisfy several conditions (16); in particular $M_1^\top M_1 + M_2^\top M_2 = I$ holds and leads to $\hat{W} = M_1^\top \hat{Q} + M_2^\top \hat{P}$. Hence Eq. (12) is rewritten as

$$\frac{d\hat{x}}{dt} = A\hat{x} + \Sigma_n C^\top \Sigma_m M_1^\top \hat{Q} + \Sigma_n C^\top \Sigma_m M_2^\top \hat{P}. \quad (23)$$

BAE is realized, if the output (22) does not contain the BA noise \hat{P} . (We will not consider the so-called variational measurement approach, in which case M_1 is frequency dependent.) In the language of linear systems theory, as stated in Eq. (8), this condition means that there is no subsystem that is controllable w.r.t. \hat{P} and observable w.r.t. y ; i.e.

$$\text{BAE: } \text{Ker}(\mathcal{C}_{\hat{P}}^\top)^c \cap \text{Range}(\mathcal{O}_y^\top) = \emptyset, \quad (24)$$

where $\mathcal{C}_{\hat{P}}$ is the controllability matrix generated from $(A, \Sigma_n C^\top \Sigma_m M_2^\top)$ and \mathcal{O}_y is the observability matrix generated from $(A, M_1 C)$. Further, again as described in Eq. (8), the condition (24) is equivalent to

$$M_1 C A^k \Sigma_n C^\top \Sigma_m M_2^\top = 0, \quad \forall k \geq 0. \quad (25)$$

Under this condition, the system equations (22) and (23) are represented in a transformed coordinate by

$$\begin{aligned} \frac{d}{dt} \begin{bmatrix} \hat{x}'_1 \\ \hat{x}'_2 \end{bmatrix} &= \begin{bmatrix} A_{11} & 0 \\ A_{21} & A_{22} \end{bmatrix} \begin{bmatrix} \hat{x}'_1 \\ \hat{x}'_2 \end{bmatrix} + \begin{bmatrix} B_{11} \\ B_{21} \end{bmatrix} \hat{Q} + \begin{bmatrix} 0 \\ B_{22} \end{bmatrix} \hat{P}, \\ y &= [C_1, 0] \begin{bmatrix} \hat{x}'_1 \\ \hat{x}'_2 \end{bmatrix} + \hat{Q}, \end{aligned}$$

showing that actually there is no signal flow from \hat{P} to y . It is also obvious from this equation that, similar to the classical case (9), the equivalent characterization to Eq. (24) in terms of the transfer function is given by

$$\text{BAE: } \Xi_{\hat{P} \rightarrow y}[s] = 0, \quad \forall s. \quad (26)$$

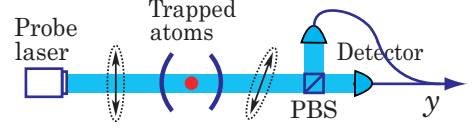


FIG. 4: Atomic ensemble under continuous measurement via Faraday rotation. PBS: polarized beam splitter.

Finally, note that achieving the above BAE condition (24) or (26) itself does not necessarily mean the improvement of signal sensitivity; actually in the case of GW force sensing discussed in Sec. VII-B, we need squeezing of the input field in addition to the BAE property for realizing such operational improvement.

B. QND

Next to see the idea of QND variables, let us here study the atomic ensemble trapped in a cavity [1, 20, 70, 71] shown in Fig. 4. The atoms couple with a probe polarized light field, via the Faraday interaction. In terms of the total energy operator \hat{J}_z and its conjugates \hat{J}_x and \hat{J}_y , which satisfy the CCRs e.g. $\hat{J}_y \hat{J}_z - \hat{J}_z \hat{J}_y = i \hat{J}_x$, the ideal dynamics of atomic ensemble is described by

$$\frac{d}{dt} \begin{bmatrix} \hat{J}_x \\ \hat{J}_y \\ \hat{J}_z \end{bmatrix} = \begin{bmatrix} -M/2 & -\sqrt{2M}\hat{P} & 0 \\ \sqrt{2M}\hat{P} & -M/2 & 0 \\ 0 & 0 & 0 \end{bmatrix} \begin{bmatrix} \hat{J}_x \\ \hat{J}_y \\ \hat{J}_z \end{bmatrix}. \quad (27)$$

\hat{P} is the phase quadrature of the input field's noise operator corresponding to the polarization, and M represents the coupling strength between the atoms and the field. In this setting, the amplitude quadrature of the output field should be measured, giving the following measurement output equation:

$$y = \hat{Q}^{\text{out}} = \sqrt{2M} \hat{J}_z + \hat{Q}.$$

From these two equations, we find that, through the Faraday interaction, the polarization of the probe field rotates depending on the total energy \hat{J}_z , but \hat{J}_z itself does not change; that is, \hat{J}_z is a QND variable that can be measured without being disturbed. Typically M is relatively small, and then the system variables obey a skew-Hermitian dynamics, implying that they preserve $\hat{J}_x^2 + \hat{J}_y^2 + \hat{J}_z^2$. Hence, in the large ensemble limit and in the short time period, the dynamics is constrained in the tangent space of this super-sphere with radius $J = N/2$ (N is the number of atoms). In particular let us set \hat{J}_x to be a constant J rather than the operator-valued variable. Then the system variables are given by the usual CCR pairs $\hat{q} = \hat{J}_y/\sqrt{J}$ and $\hat{p} = \hat{J}_z/\sqrt{J}$ satisfying $\hat{q}\hat{p} - \hat{p}\hat{q} = i$, and the above system dynamics can be simplified to the following linear equation:

$$\frac{d}{dt} \begin{bmatrix} \hat{q} \\ \hat{p} \end{bmatrix} = \sqrt{\mu} \begin{bmatrix} 1 \\ 0 \end{bmatrix} \hat{P}, \quad y = \sqrt{\mu} \hat{p} + \hat{Q},$$

where $\mu = 2MJ$. Clearly, \hat{p} is not disturbed by the noise while it appears in the output signal, thus \hat{p} is a QND variable. A merit of QND measurement is in the application to state preparation; if a QND variable exists, it is sometimes possible to deterministically stabilize its eigenstate by feedback [1], which can be highly non-classical such as a spin-squeezed state [20, 70].

As in the BAE case, we have a general characterization of the linear system (12) and (15) having a QND variable. Let $\hat{r} = v^\top \hat{x}$ be a QND variable with $v \in \mathbb{R}^{2n}$. Then, by definition, \hat{r} must not be affected by the input field \hat{W} , while it appears in the output signal (15), $y = MC\hat{x} + M\hat{W}$. This means that, in the language of linear systems theory, $\hat{r} = v^\top \hat{x}$ is uncontrollable w.r.t. \hat{W} and observable w.r.t. y . Thus, the iff condition for a QND variable to exist is given by

$$\text{QND: } \text{Ker}(\mathcal{C}_{\hat{W}}^\top) \cap \text{Range}(\mathcal{O}_y^\top) \neq \emptyset, \quad (28)$$

and the vector v lives in this intersection. Here, $\mathcal{C}_{\hat{W}}$ and \mathcal{O}_y are the controllability and observability matrices of the system (12) and (15). Note that the condition $v \in \text{Ker}(\mathcal{C}_{\hat{W}}^\top)$ can be explicitly represented by

$$v^\top A^k \Sigma_n C^\top = 0, \quad \forall k \geq 0. \quad (29)$$

Now let us collect QND variables into a single vector \hat{x}'_2 . Then, as described in Sec. II-A, \hat{x}'_2 constitutes an uncontrollable subsystem w.r.t. \hat{W} , which can be clearly seen in the transformed coordinate:

$$\begin{aligned} \frac{d}{dt} \begin{bmatrix} \hat{x}'_1 \\ \hat{x}'_2 \end{bmatrix} &= \begin{bmatrix} A_{11} & A_{12} \\ 0 & A_{22} \end{bmatrix} \begin{bmatrix} \hat{x}'_1 \\ \hat{x}'_2 \end{bmatrix} + \begin{bmatrix} B_1 \\ 0 \end{bmatrix} \hat{W}, \\ y &= [C_1, C_2] \begin{bmatrix} \hat{x}'_1 \\ \hat{x}'_2 \end{bmatrix} + M\hat{W}. \end{aligned}$$

Note $C_2 \neq 0$ due to the observability condition. Hence, \hat{x}'_2 is free from \hat{W} , while it appears in y . Remarkably, \hat{x}'_2 obeys the closed dynamics $d\hat{x}'_2/dt = A_{22}\hat{x}'_2$; thus \hat{x}'_2 is a generalization of a standard QND variable, which is usually considered to be static (i.e. $\hat{x}'_2(t) = \hat{x}'_2(0)$, $\forall t$); see [72] for further detailed discussion. The above equation now enables us to obtain the equivalent condition to Eq. (28) in terms of the transfer functions:

$$\text{QND: } \Xi_{\hat{W} \rightarrow \hat{x}'_2}[s] = 0, \quad \forall s \quad \& \quad \Xi_{\hat{x}'_2 \rightarrow y}[s] \neq 0, \quad \exists s. \quad (30)$$

C. DFS

The idea of the third control goal, generation of a DFS, can be clearly seen from the work [61], which studies a quantum memory served by an atomic ensemble in a cavity. Each atom has Λ -type energy levels, constituted by two metastable ground states ($|s\rangle, |g\rangle$) and an excited state $|e\rangle$. The state transition between $|e\rangle$ and $|g\rangle$ is naturally coupled to the cavity mode \hat{a}_1 with strength $g\sqrt{N}$ (N denotes the number of atoms), while the $|s\rangle \leftrightarrow |e\rangle$

transition is induced by a classical magnetic field with time-varying Rabi frequency $\omega(t)$. The system variables are the polarization operator $\hat{a}_2 = \hat{\sigma}_{ge}/\sqrt{N}$ and the spin-wave operator $\hat{a}_3 = \hat{\sigma}_{gs}/\sqrt{N}$, where $\hat{\sigma}_\bullet$ is the collective lowering operator; in a large ensemble limit, they can be well approximated by annihilation operators. Consequently the system dynamics is given by

$$\begin{aligned} \frac{d}{dt} \begin{bmatrix} \hat{a}_1 \\ \hat{a}_2 \\ \hat{a}_3 \end{bmatrix} &= \begin{bmatrix} -\kappa & ig\sqrt{N} & 0 \\ ig\sqrt{N} & -i\delta & i\omega \\ 0 & i\omega^* & 0 \end{bmatrix} \begin{bmatrix} \hat{a}_1 \\ \hat{a}_2 \\ \hat{a}_3 \end{bmatrix} - \begin{bmatrix} \sqrt{2\kappa} \\ 0 \\ 0 \end{bmatrix} \hat{A}, \\ \hat{A}^{\text{out}} &= \sqrt{2\kappa}\hat{a}_1 + \hat{A}, \end{aligned} \quad (31)$$

where κ denotes the cavity decay rate and δ is the detuning between the cavity center frequency and the $|s\rangle \leftrightarrow |e\rangle$ transition frequency. This system works as a quantum memory in the following way. First, a state to be stored is carried by an appropriately shaped optical pulse on the input field \hat{A} , and it is transferred to the metastable state $|s\rangle$; the Rabi frequency $\omega(t)$ is suitably designed throughout this writing process. In the storage stage, the classical magnetic field is turned off, i.e. $\omega(t) = 0$. It is seen from Eq. (31) that the spin-wave operator \hat{a}_3 is then completely decoupled from the fields \hat{A} and \hat{A}^{out} ; that is, \hat{a}_3 constitutes a linear DFS, and ideally its state is perfectly preserved. In the language of systems theory, this DFS is uncontrollable w.r.t. \hat{A} and unobservable w.r.t. \hat{A}^{out} . Note that \hat{a}_3 is not a variable on the so-called decoherence-free subspace, which though has the same abbreviation. In general, if the system's Hilbert space can be decomposed to $(\mathcal{H}_1 \otimes \mathcal{H}_2) \oplus \mathcal{H}_3$ and \mathcal{H}_1 is free from external noise, then it is called the DF subsystem and particularly when $\dim \mathcal{H}_2 = 1$ it is called the DF subspace [41, 42]; now we are dealing with the case where \hat{a}_3 and (\hat{a}_1, \hat{a}_2) live in \mathcal{H}_1 and \mathcal{H}_2 , respectively, while $\dim \mathcal{H}_3 = 0$. For other examples of such an infinite dimensional DFS, see [53, 54, 55, 69, 73, 74, 75].

The above fact reasonably leads to a general characterization of the system (12) and (14) that contains a DFS. By definition, a DFS is completely decoupled from the probe/environment field, so it is not affected by \hat{W} and also it does not appear in \hat{W}^{out} . In the language of systems theory, a variable contained in the DFS is uncontrollable w.r.t. \hat{W} and unobservable w.r.t. \hat{W}^{out} . Thus the iff condition for a DFS to exist is given by

$$\text{DFS: } \text{Ker}(\mathcal{C}_{\hat{W}}^\top) \cap \text{Range}(\mathcal{O}_{\hat{W}^{\text{out}}}^\top)^c \neq \emptyset, \quad (32)$$

where $\mathcal{C}_{\hat{W}}$ and $\mathcal{O}_{\hat{W}^{\text{out}}}$ are the controllability and observability matrices of the system (12) and (14). In particular, as seen in Eqs. (4) and (7), there always exists a coordinate transformation such that $\hat{r} = v^\top \hat{x}$ is a variable of the DFS iff the vector $v \in \mathbb{R}^{2n}$ is contained in the intersection $\text{Ker}(\mathcal{C}_{\hat{W}}^\top) \cap \text{Ker}(\mathcal{O}_{\hat{W}^{\text{out}}}^\top)$; that is, it satisfies

$$v^\top A^k \Sigma_n C^\top \Sigma_m = 0, \quad C A^k v = 0, \quad \forall k \geq 0. \quad (33)$$

(A convenient method to construct such v is given in [75].) Then, as in the QND case, by collecting all variables in the DFS into a single vector \hat{x}'_2 , we find that the

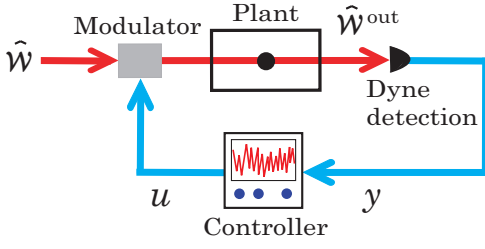


FIG. 5: General configuration of the type-1 MF control.

system equations can be transformed to

$$\begin{aligned} \frac{d}{dt} \begin{bmatrix} \hat{x}'_1 \\ \hat{x}'_2 \end{bmatrix} &= \begin{bmatrix} A_{11} & 0 \\ 0 & A_{22} \end{bmatrix} \begin{bmatrix} \hat{x}'_1 \\ \hat{x}'_2 \end{bmatrix} + \begin{bmatrix} B_1 \\ 0 \end{bmatrix} \hat{W}, \\ \hat{W}^{\text{out}} &= [C_1, 0] \begin{bmatrix} \hat{x}'_1 \\ \hat{x}'_2 \end{bmatrix} + \hat{W}. \end{aligned}$$

Thus \hat{x}'_2 obeys the closed-dynamics $d\hat{x}'_2/dt = A_{22}\hat{x}'_2$; especially if $A_{22} = 0$, the state of \hat{x}'_2 is kept unchanged, and the DFS works as a memory. Lastly, the condition for \hat{x}'_2 to be a variable in the DFS is given in terms of the transfer functions by

$$\text{DFS: } \Xi_{\hat{W} \rightarrow \hat{x}'_2}[s] = 0, \quad \Xi_{\hat{x}'_2 \rightarrow \hat{W}^{\text{out}}}[s] = 0, \quad \forall s. \quad (34)$$

Note here again that the condition (32) or (34) is only a necessary requirement for the system to have a good memory architecture, and it itself does not lead to the improvement of memory retrieval fidelity. To realize a high-quality quantum memory process, in addition to engineering such a DFS, we need a sophisticated method for transferring an input state to the memory part. For instance by suitable pulse shaping of the input wave packet, lossless state transfer to a general linear DFS and accordingly perfect memory fidelity can be achieved [69].

IV. THE NO-GO THEOREMS: TYPE-1 CASE

In this paper, we study a general linear system having multi input and multi output fields (it is called a MIMO system). The first essential question is about which input and output fields should be used for feedback. We define the *type-1 control* as a configuration where at most all the input and output fields can be used for this purpose. Note that, if the system has single input-output channel such as the one shown in Sec. II-C (ii), the control configuration must be of type-1. Figure 5 illustrates the general configuration of type-1 MF control. That is, at most all the plant's output fields can be measured, and the measurement results $y(t)$ are then processed in a classical system (controller) that produces a control signal $u(t)$. From the standpoint comparing MF and CF, we assume that the control is carried out by modulating the input probe fields, which can be physically implemented using an electric optical modulator on the optical field; in

the type-1 case, hence, at most all the plant's input fields can be modulated using the control signal $u(t)$. This section studies the type-1 MF control and shows the no-go theorems given in the left column of Table I.

A. The closed-loop system with type-1 MF

As described above, the MF control is carried out by modulating the input probe fields. This mathematically means that the input field is replaced by $\hat{W} + u$, where $u = [u_1, \dots, u_{2m}]^T$ is a vector of classical control signals representing the modulation. Hence our plant system is now given by

$$\frac{d\hat{x}}{dt} = A\hat{x} + \Sigma_n C^T \Sigma_m (\hat{W} + u), \quad (35)$$

$$\hat{W}^{\text{out}} = C\hat{x} + \hat{W} + u. \quad (36)$$

Note that the output field is directly controlled. (In what follows we omit the subscript of Σ_\bullet for notational simplicity.) The output signal is obtained by measuring \hat{W}^{out} :

$$y = M_1 \hat{W}^{\text{out}} = M_1 C \hat{x} + \hat{Q} + M_1 u, \quad (37)$$

where $\hat{Q} = M_1 \hat{W}$ with M_1 the symplectic matrix defined in Sec. II-B. Also the conjugate noise operator is given by $\hat{P} = M_2 \hat{W}$; these matrices satisfy the conditions (16).

The controller is a classical system that processes the measurement result $y(t)$ and produces the control signal $u(t)$. The dynamical equation of this system can be generally represented by

$$\frac{dx_K}{dt} = A_K x_K + B_K y, \quad u = C_K x_K, \quad (38)$$

where (A_K, B_K, C_K) are the parameter matrices to be designed. x_K is the vector of controller's variables, and its dimension is also a parameter; hence there is a large freedom in engineering the controller. Note that the matrices are not necessarily of full rank, meaning that in this case some output fields are not measured or some input fields are not modulated. Combining all the above equations, we have the closed-loop (quantum-classical hybrid) dynamics of $\hat{x}_e = [\hat{x}^T, x_K^T]^T$ as follows;

$$\begin{aligned} \frac{d\hat{x}_e}{dt} &= \begin{bmatrix} A & \Sigma C^T \Sigma C_K \\ B_K M_1 C & A_K + B_K M_1 C_K \end{bmatrix} \hat{x}_e \\ &\quad + \begin{bmatrix} \Sigma C^T \Sigma \\ B_K M_1 \end{bmatrix} \hat{W}, \end{aligned} \quad (39)$$

$$y = [M_1 C, M_1 C_K] \hat{x}_e + \hat{Q}. \quad (40)$$

Hence, \hat{Q} is the shot noise. Equation (39) can be expressed in terms of the quadratures \hat{Q} and \hat{P} as:

$$\begin{aligned} \frac{d\hat{x}_e}{dt} &= \begin{bmatrix} A & \Sigma C^T \Sigma C_K \\ B_K M_1 C & A_K + B_K M_1 C_K \end{bmatrix} \hat{x}_e \\ &\quad + \begin{bmatrix} \Sigma C^T \Sigma M_1^T \\ B_K \end{bmatrix} \hat{Q} + \begin{bmatrix} \Sigma C^T \Sigma M_2^T \\ 0 \end{bmatrix} \hat{P}, \end{aligned} \quad (41)$$

due to $\hat{\mathcal{W}} = M_1^\top \hat{\mathcal{Q}} + M_2^\top \hat{\mathcal{P}}$. We aim to find a set of matrices $(A_K, B_K, C_K, M_1, M_2)$ that achieves the control goals described in Sec. III; but as shown below, it is impossible to accomplish those tasks.

B. BAE

Suppose that BAE holds for the closed-loop dynamics (41) with output (40); that is, the condition (24) holds for this system, which is now $\text{Ker}(\mathcal{C}_{\hat{\mathcal{P}}}^\top) \cap \text{Range}(\mathcal{O}_y^\top) = \emptyset$. (Equivalently, the transfer function of the closed-loop system satisfies $\Xi_{\hat{\mathcal{P}} \rightarrow y}^{(fb)}[s] = 0, \forall s$.) This is further equivalent, as implied by Eq. (25), to

$$[M_1 C, M_1 C_K] \begin{bmatrix} A & \Sigma C^\top \Sigma C_K \\ B_K M_1 C & A_K + B_K M_1 C_K \end{bmatrix}^k \times \begin{bmatrix} \Sigma C^\top \Sigma M_2^\top \\ 0 \end{bmatrix} = 0, \quad \forall k \geq 0. \quad (42)$$

First, the case $k = 0$ leads to $M_1 C \Sigma C^\top \Sigma M_2^\top = 0$. Then, using this condition, we find that the case $k = 1$ yields $M_1 C A \Sigma C^\top \Sigma M_2^\top = 0$. This further allows us from the case $k = 2$ to have $M_1 C A^2 \Sigma C^\top \Sigma M_2^\top = 0$. Repeating the same procedure we eventually obtain

$$M_1 C A^k \Sigma C^\top \Sigma M_2^\top = 0, \quad \forall k \geq 0.$$

This is exactly the BAE condition for the *original* plant system (22) and (23), i.e.

$$\frac{d\hat{x}}{dt} = A\hat{x} + \Sigma C^\top \Sigma M_1^\top \hat{\mathcal{Q}} + \Sigma C^\top \Sigma M_2^\top \hat{\mathcal{P}}, \quad y = M_1 C \hat{x} + \hat{\mathcal{Q}}.$$

Equivalently, the transfer function of the original plant system satisfies $\Xi_{\hat{\mathcal{P}} \rightarrow y}^{(o)}[s] = 0, \forall s$. Thus the contrapositive of this result yields the following theorem.

Theorem 1: If the original plant system does not have the BAE property, then, any type-1 MF control cannot realize BAE for the closed-loop system.

C. QND

First of all, let us consider the case where the closed-loop system (39) and (40) has a QND variable \hat{r} . This should be “purely quantum”, meaning that \hat{r} is composed of only the quantum variables $\hat{x} = [\hat{q}_1, \hat{p}_1, \dots, \hat{q}_n, \hat{p}_n]^\top$; hence it is of the form $\hat{r} = v^\top \hat{x} = \tilde{v}^\top \hat{x}_e$ with $\tilde{v} = [v^\top, 0^\top]^\top$. As described in Eq. (28), this means $\tilde{v} \in \text{Ker}(\mathcal{C}_{\hat{\mathcal{W}}}^\top) \cap \text{Range}(\mathcal{O}_y^\top)$, with $\mathcal{C}_{\hat{\mathcal{W}}}$ and \mathcal{O}_y the controllability and observability matrices of the system (39) and (40). To prove the no-go theorem, the following two facts are useful. First, $\tilde{v} \in \text{Ker}(\mathcal{C}_{\hat{\mathcal{W}}}^\top)$ means that

$$[v^\top, 0^\top] \begin{bmatrix} A & \Sigma C^\top \Sigma C_K \\ B_K M_1 C & A_K + B_K M_1 C_K \end{bmatrix}^k \begin{bmatrix} \Sigma C^\top \Sigma \\ B_K M_1 \end{bmatrix} = 0,$$

for all $k \geq 0$. It follows from a similar procedure as in the BAE case that this is equivalent to $v^\top A^k \Sigma C^\top \Sigma = 0, \forall k \geq 0$; i.e. $v \in \text{Ker}(\mathcal{C}_{\hat{\mathcal{W}}}^\top)$ with $\mathcal{C}_{\hat{\mathcal{W}}}$ the controllability matrix of the *original* plant system (12) and (15). Second, $\tilde{v} \in \text{Ker}(\mathcal{O}_y)$ is expressed by

$$[M_1 C, M_1 C_K] \begin{bmatrix} A & \Sigma C^\top \Sigma C_K \\ B_K M_1 C & A_K + B_K M_1 C_K \end{bmatrix}^k \begin{bmatrix} v \\ 0 \end{bmatrix} = 0$$

for all $k \geq 0$. This is equivalent to $M_1 C A^k v = 0, \forall k \geq 0$, meaning that $v \in \text{Ker}(\mathcal{O}_y)$ for the original plant system.

Now we prove the theorem. Suppose that the original plant system (12) and (15) does not have a QND variable; hence for any variable $\hat{r} = v^\top \hat{x}$, the vector v satisfies $v \in \text{Ker}(\mathcal{C}_{\hat{\mathcal{W}}}^\top)^c$ or $v \in \text{Range}(\mathcal{O}_y^\top)^c$ for the original plant system. In particular, since the unobservability property does not depend on the choice of a specific coordinate, the latter condition is equivalently converted to $v \in \text{Ker}(\mathcal{O}_y)$. But as proven above, these two conditions are equivalent to $\tilde{v} \in \text{Ker}(\mathcal{C}_{\hat{\mathcal{W}}}^\top)^c$ or $\tilde{v} \in \text{Ker}(\mathcal{O}_y)$ for the closed-loop system; that is, the closed-loop system does not have a QND variable of the form $\hat{r} = v^\top \hat{x} = \tilde{v}^\top \hat{x}_e$. Thus the following result is obtained.

Theorem 2: If the original plant system does not have a QND variable, then, any type-1 MF control cannot generate a QND variable in the closed-loop system.

D. DFS

Finally we prove the no-go theorem for generating a DFS via the type-1 MF control. Let us assume that the closed-loop dynamics (39) with the output field

$$\hat{\mathcal{W}}^{\text{out}} = [C, C_K] \begin{bmatrix} \hat{x} \\ x_K \end{bmatrix} + \hat{\mathcal{W}}$$

contains a DFS composed of “purely quantum” variables of the form $\hat{r} = v^\top \hat{x} = \tilde{v}^\top \hat{x}_e$. Then, it follows from the statement below Eq. (32) that $\tilde{v} \in \text{Ker}(\mathcal{C}_{\hat{\mathcal{W}}}^\top)$ and $\tilde{v} \in \text{Ker}(\mathcal{O}_{\hat{\mathcal{W}}^{\text{out}}})$ hold. As proven in the QND case, the first condition equivalently leads to $v \in \text{Ker}(\mathcal{C}_{\hat{\mathcal{W}}}^\top)$ for the original plant system (12) and (14). Also in almost the same way we can prove that the second condition is equivalent to $v \in \text{Ker}(\mathcal{O}_{\hat{\mathcal{W}}^{\text{out}}})$ for the original plant system. These two conditions on v mean that the original plant system (12) and (14) has a DFS, thus the contrapositive yields the following theorem.

Theorem 3: If the original plant system does not have a DFS, then, any type-1 MF control cannot generate a DFS in the closed-loop system.

V. THE NO-GO THEOREMS: TYPE-2 CASE

In the type-1 case, it is assumed that at most all the plant’s output fields can be used for feedback control and they are equally evaluated. For example, in the type-1

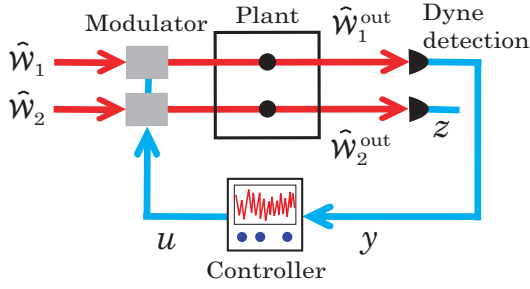


FIG. 6: General configuration of the type-2 MF control.

BAE case, the BA noise $\hat{\mathcal{P}}$ must not appear in *all* the elements of y . But it is sometimes more reasonable to give different roles to the output fields; such a control schematic in the MF case is illustrated in Fig. 6, which we call the *type-2 control* configuration. In this case, at most all the components of $\hat{\mathcal{W}}_1^{\text{out}}$ can be used for feedback control, while those of $\hat{\mathcal{W}}_2^{\text{out}}$ are for evaluation; that is, they will be measured to extract some information about the system or will be kept untouched for later use. For instance, we attempt to design a MF control based on the measurement of $\hat{\mathcal{W}}_1^{\text{out}}$, so that the BA noise does not appear in the measurement output of $\hat{\mathcal{W}}_2^{\text{out}}$. However, we will see that such a MF control strategy does not work to achieve any of the control goals. That is, in this section, the type-2 no-go theorems in Table I will be proven.

A. The closed-loop system with type-2 MF

As in the case of type-1 control, we study the situation where the feedback control is performed by modulating the input fields. The plant system driven by the modulated fields obeys the following dynamical equation:

$$\begin{aligned} \frac{d\hat{x}}{dt} &= A\hat{x} + \Sigma C_1^\top \Sigma (\hat{\mathcal{W}}_1 + u_1) + \Sigma C_2^\top \Sigma (\hat{\mathcal{W}}_2 + u_2), \\ \hat{\mathcal{W}}_1^{\text{out}} &= C_1 \hat{x} + \hat{\mathcal{W}}_1 + u_1, \quad \hat{\mathcal{W}}_2^{\text{out}} = C_2 \hat{x} + \hat{\mathcal{W}}_2 + u_2. \end{aligned}$$

u_1 and u_2 are the vectors of control signals that represent the time-varying amplitude of the input fields $\hat{\mathcal{W}}_1$ and $\hat{\mathcal{W}}_2$, respectively. Note that in general the size of C_1 and C_2 need not to be equal. The output field $\hat{\mathcal{W}}_1^{\text{out}}$ is measured by a set of dyne detectors, which yield

$$y = M\hat{\mathcal{W}}_1^{\text{out}} = MC_1\hat{x} + M\hat{\mathcal{W}}_1 + Mu_1.$$

M is the symplectic matrix, representing which quadratures of $\hat{\mathcal{W}}_1^{\text{out}}$ is measured. The measurement result $y(t)$ is sent to a classical feedback controller of the form

$$\frac{dx_K}{dt} = A_K x_K + B_K y, \quad u_1 = C_{K1} x_K, \quad u_2 = C_{K2} x_K.$$

Note that u_2 is allowed to contain the direct term from y , i.e. $u_2 = C_{K2} x_K + D_K y$; but this modification does not change the results shown below, thus for simplicity we

assume $D_K = 0$. Combining all the above equations, we end up with the closed-loop dynamics of $\hat{x}_e = [\hat{x}^\top, x_K^\top]^\top$:

$$\begin{aligned} \frac{d\hat{x}_e}{dt} &= \begin{bmatrix} A & \Sigma C_1^\top \Sigma C_{K1} + \Sigma C_2^\top \Sigma C_{K2} \\ B_K M C_1 & A_K + B_K M C_{K1} \end{bmatrix} \hat{x}_e \\ &\quad + \begin{bmatrix} \Sigma C_1^\top \Sigma \\ B_K M \end{bmatrix} \hat{\mathcal{W}}_1 + \begin{bmatrix} \Sigma C_2^\top \Sigma \\ 0 \end{bmatrix} \hat{\mathcal{W}}_2. \end{aligned} \quad (43)$$

There are two kinds of output signals of the system. One is $y(t)$, which is used for feedback control. Due to the direct control term, it is now of the form

$$y = [MC_1, MC_{K1}] \hat{x}_e + M\hat{\mathcal{W}}_1. \quad (44)$$

The other one is used for evaluation, which is obtained by measuring the second output field $\hat{\mathcal{W}}_2^{\text{out}}$:

$$z = M_1 \hat{\mathcal{W}}_2^{\text{out}} = [M_1 C_2, M_1 C_{K2}] \hat{x}_e + \hat{\mathcal{Q}}, \quad (45)$$

where we have defined $\hat{\mathcal{Q}} = M_1 \hat{\mathcal{W}}_2$.

B. BAE

The goal of BAE is to evade the BA noise so that it does not appear in the output signal (45). Now $\hat{\mathcal{Q}} = M_1 \hat{\mathcal{W}}_2$ is the unavoidable shot noise and $\hat{\mathcal{P}} := M_2 \hat{\mathcal{W}}_2$ is the BA noise, where the matrices satisfy Eq. (16). Note that the noise term of the closed-loop system (43) can be expressed by

$$\begin{aligned} &\text{noise term of Eq. (43)} \\ &= \begin{bmatrix} \Sigma C_1^\top \Sigma \\ B_K M \end{bmatrix} \hat{\mathcal{W}}_1 + \begin{bmatrix} \Sigma C_2^\top \Sigma M_1^\top \\ 0 \end{bmatrix} \hat{\mathcal{Q}} + \begin{bmatrix} \Sigma C_2^\top \Sigma M_2^\top \\ 0 \end{bmatrix} \hat{\mathcal{P}}. \end{aligned}$$

Also the original system without control is given by

$$\begin{aligned} \frac{d\hat{x}}{dt} &= A\hat{x} + \Sigma C_1^\top \Sigma \hat{\mathcal{W}}_1 + \Sigma C_2^\top \Sigma (M_1^\top \hat{\mathcal{Q}} + M_2^\top \hat{\mathcal{P}}), \\ y &= MC_1 \hat{x} + M\hat{\mathcal{W}}_1, \quad z = M_1 C_2 \hat{x} + \hat{\mathcal{Q}}. \end{aligned} \quad (46)$$

We start with the assumption that BAE holds for the closed-loop system (43) and (45). In terms of the transfer function, this means that $\Xi_{\hat{\mathcal{W}}_1 \rightarrow z}^{(fb)}[s] = 0$ and $\Xi_{\hat{\mathcal{P}} \rightarrow z}^{(fb)}[s] = 0$ are satisfied for all s , for this system (see Eq. (26)). Thus, the Laplace transform of $z(t)$ is given by

$$\begin{aligned} z[s] &= \Xi_{\hat{\mathcal{Q}} \rightarrow z}^{(fb)}[s] \hat{\mathcal{Q}}[s] + \Xi_{\hat{\mathcal{P}} \rightarrow z}^{(fb)}[s] \hat{\mathcal{P}}[s] + \Xi_{\hat{\mathcal{W}}_1 \rightarrow z}^{(fb)}[s] \hat{\mathcal{W}}_1[s] \\ &= \Xi_{\hat{\mathcal{Q}} \rightarrow z}^{(fb)}[s] \hat{\mathcal{Q}}[s]. \end{aligned}$$

Let us now focus on the Laplace transform of $y(t)$:

$$y[s] = \Xi_{\hat{\mathcal{Q}} \rightarrow y}^{(fb)}[s] \hat{\mathcal{Q}}[s] + \Xi_{\hat{\mathcal{P}} \rightarrow y}^{(fb)}[s] \hat{\mathcal{P}}[s] + \Xi_{\hat{\mathcal{W}}_1 \rightarrow y}^{(fb)}[s] \hat{\mathcal{W}}_1[s].$$

Both $z[s]$ and $y[s]$ are vectors of classical numbers, hence all their components commute with each other; i.e., $zy^\top - (yz^\top)^\top = 0$ holds. Then, since in the Laplace domain the

CCRs are represented by $[\hat{Q}_j, \hat{P}_k] = \delta_{jk}i/2s$, $[\hat{Q}_j, \hat{Q}_k] = 0$, and $[\hat{Q}_j, \hat{W}_{1,k}] = 0$, we have

$$\begin{aligned} & zy^\top - (yz^\top)^\top \\ &= \Xi_{\hat{Q} \rightarrow z}^{(fb)} \hat{Q} \hat{P}^\top (\Xi_{\hat{P} \rightarrow y}^{(fb)})^\top - \left[\Xi_{\hat{P} \rightarrow y}^{(fb)} \hat{P} \hat{Q}^\top (\Xi_{\hat{Q} \rightarrow z}^{(fb)})^\top \right]^\top \\ &= \Xi_{\hat{Q} \rightarrow z}^{(fb)} \left[\hat{Q} \hat{P}^\top - (\hat{P} \hat{Q}^\top)^\top \right] (\Xi_{\hat{P} \rightarrow y}^{(fb)})^\top \\ &= \frac{i}{2s} \Xi_{\hat{Q} \rightarrow z}^{(fb)} (\Xi_{\hat{P} \rightarrow y}^{(fb)})^\top = 0. \end{aligned}$$

But Eq. (45) clearly indicates that $\Xi_{\hat{Q} \rightarrow z}^{(fb)}[s]$ is invertible for all s , hence we conclude $\Xi_{\hat{P} \rightarrow y}^{(fb)}[s] = 0$, $\forall s$. This equivalently leads to the following set of equalities:

$$\begin{aligned} [MC_1, MC_{K1}] & \begin{bmatrix} A & \Sigma C_1^\top \Sigma C_{K1} + \Sigma C_2^\top \Sigma C_{K2} \\ B_K MC_1 & A_K + B_K MC_{K1} \end{bmatrix}^k \\ & \times \begin{bmatrix} \Sigma C_2^\top \Sigma M_2^\top \\ 0 \end{bmatrix} = 0, \quad \forall k \geq 0. \end{aligned}$$

Likewise the proof in the type-1 case, we have

$$MC_1 A^k \Sigma C_2^\top \Sigma M_2^\top = 0, \quad \forall k \geq 0, \quad (47)$$

which implies that the original system (46) satisfies $\Xi_{\hat{P} \rightarrow y}^{(o)}[s] = 0$, $\forall s$. Now the BAE condition $\Xi_{\hat{P} \rightarrow z}^{(fb)}[s] = 0$, $\forall s$ is expressed in the state space representation by

$$\begin{aligned} [M_1 C_2, M_1 C_{K2}] & \begin{bmatrix} A & \Sigma C_1^\top \Sigma C_{K1} + \Sigma C_2^\top \Sigma C_{K2} \\ B_K MC_1 & A_K + B_K MC_{K1} \end{bmatrix}^k \\ & \times \begin{bmatrix} \Sigma C_2^\top \Sigma M_2^\top \\ 0 \end{bmatrix} = 0, \quad \forall k \geq 0. \end{aligned}$$

Then, using Eq. (47), we deduce

$$M_1 C_2 A^k \Sigma C_2^\top \Sigma M_2^\top = 0, \quad \forall k \geq 0.$$

Hence, for the original system (46), the transfer function from \hat{P} to z is zero; i.e., $\Xi_{\hat{P} \rightarrow z}^{(o)}[s] = 0$, $\forall s$.

We finally prove $\Xi_{\hat{W}_1 \rightarrow z}^{(o)}[s] = 0$, $\forall s$. The above result implies $z^{(o)}[s] = \Xi_{\hat{W}_1 \rightarrow z}^{(o)}[s] \hat{W}_1[s] + \Xi_{\hat{Q} \rightarrow z}^{(o)}[s] \hat{Q}[s]$. Moreover, from Eq. (47) we have $\Xi_{\hat{P} \rightarrow y}^{(o)}[s] = 0$, $\forall s$, which leads to $y^{(o)}[s] = \Xi_{\hat{W}_1 \rightarrow y}^{(o)}[s] \hat{W}_1[s] + \Xi_{\hat{Q} \rightarrow y}^{(o)}[s] \hat{Q}[s]$. Then, since both $y^{(o)}[s]$ and $z^{(o)}[s]$ are c-numbers, we have

$$\begin{aligned} & y^{(o)} z^{(o)\top} - (z^{(o)} y^{(o)\top})^\top = \Xi_{\hat{W}_1 \rightarrow y}^{(o)} \hat{W}_1 \hat{W}_1^\top (\Xi_{\hat{W}_1 \rightarrow z}^{(o)})^\top \\ & \quad - \left[\Xi_{\hat{W}_1 \rightarrow z}^{(o)} \hat{W}_1 \hat{W}_1^\top (\Xi_{\hat{W}_1 \rightarrow y}^{(o)})^\top \right]^\top \\ &= \Xi_{\hat{W}_1 \rightarrow y}^{(o)} \left[\hat{W}_1 \hat{W}_1^\top - (\hat{W}_1 \hat{W}_1^\top)^\top \right] (\Xi_{\hat{W}_1 \rightarrow z}^{(o)})^\top \\ &= \frac{i}{2s} \Xi_{\hat{W}_1 \rightarrow y}^{(o)} \Sigma (\Xi_{\hat{W}_1 \rightarrow z}^{(o)})^\top = 0. \end{aligned}$$

Note now that $\Xi_{\hat{W}_1 \rightarrow z}^{(o)}[s]$ does not depend on the matrix M , representing which quadratures of \hat{W}_1^{out} are measured. This means that the above equality holds for other choice of measurement, say $\tilde{y} = \tilde{M} \hat{W}_1$. Thus we have

$$\begin{aligned} & \begin{bmatrix} \Xi_{\hat{W}_1 \rightarrow y}^{(o)} \\ \Xi_{\hat{W}_1 \rightarrow \tilde{y}}^{(o)} \end{bmatrix} \Sigma (\Xi_{\hat{W}_1 \rightarrow z}^{(o)})^\top = \begin{bmatrix} M \\ \tilde{M} \end{bmatrix} \Xi_{\hat{W}_1 \rightarrow \hat{W}_1^{\text{out}}}^{(o)} \Sigma (\Xi_{\hat{W}_1 \rightarrow z}^{(o)})^\top \\ &= 0. \end{aligned}$$

\tilde{M} is chosen so that $[M^\top, \tilde{M}^\top]$ is invertible. Because $\Xi_{\hat{W}_1 \rightarrow \hat{W}_1^{\text{out}}}^{(o)}[s]$ is also invertible, $\Xi_{\hat{W}_1 \rightarrow z}^{(o)}[s] = 0$, $\forall s$. Together with the above result $\Xi_{\hat{P} \rightarrow z}^{(o)}[s] = 0$, $\forall s$, this means that BAE holds for the original plant system (46). Consequently, we have the following result:

Theorem 4: If the original plant system does not have the BAE property, then, any type-2 MF control cannot realize BAE for the closed-loop system.

C. QND

The idea for the proof is the same as that taken in the type-1 case. Again, a QND variable is of the form $\hat{r} = v^\top \hat{x} = \tilde{v}^\top \hat{x}_e$ with $\tilde{v} = [v^\top, 0^\top]^\top$. Now the closed-loop system is given by Eqs. (43), (44), and (45), showing that it is subjected to the input noise field $[\hat{W}_1^\top, \hat{W}_2^\top]^\top$ and it generates the measurement outputs $[y^\top, z^\top]^\top$. Thus by definition \hat{r} is a QND variable iff $\tilde{v} \in \text{Ker}(\mathcal{C}_{\hat{W}_1}^\top) \cap \text{Ker}(\mathcal{C}_{\hat{W}_2}^\top)$ and $\tilde{v} \in \text{Range}(\mathcal{O}_y^\top) \cup \text{Range}(\mathcal{O}_z^\top)$. The former condition means that

$$\begin{aligned} & [v^\top, 0^\top] \begin{bmatrix} A & \Sigma C_1^\top \Sigma C_{K1} + \Sigma C_2^\top \Sigma C_{K2} \\ B_K MC_1 & A_K + B_K MC_{K1} \end{bmatrix}^k \\ & \times \begin{bmatrix} \Sigma C_1^\top \Sigma & \Sigma C_2^\top \Sigma \\ B_K M & 0 \end{bmatrix} = 0, \quad \forall k \geq 0. \end{aligned}$$

This is equivalent to $v^\top A^k \Sigma C_1^\top \Sigma = 0$ and $v^\top A^k \Sigma C_2^\top \Sigma = 0$ for all $k \geq 0$; that is, $v \in \text{Ker}(\mathcal{C}_{\hat{W}_1}^\top) \cap \text{Ker}(\mathcal{C}_{\hat{W}_2}^\top)$ holds for the original plant system (46). (Note $\hat{W}_2 = M_1^\top \hat{Q} + M_2^\top \hat{P}$.) Related to the latter one, let us consider the condition $\tilde{v} \in \text{Ker}(\mathcal{O}_y) \cap \text{Ker}(\mathcal{O}_z)$. This is expressed by

$$\begin{aligned} & \begin{bmatrix} MC_1 & MC_{K1} \\ M_1 C_2 & M_1 C_{K2} \end{bmatrix} \\ & \times \begin{bmatrix} A & \Sigma C_1^\top \Sigma C_{K1} + \Sigma C_2^\top \Sigma C_{K2} \\ B_K MC_1 & A_K + B_K MC_{K1} \end{bmatrix}^k \begin{bmatrix} v \\ 0 \end{bmatrix} = 0, \end{aligned}$$

for all $k \geq 0$, which equivalently leads to

$$\begin{bmatrix} MC_1 \\ M_1 C_2 \end{bmatrix} A^k v = 0, \quad \forall k \geq 0.$$

Thus $v \in \text{Ker}(\mathcal{O}_y) \cap \text{Ker}(\mathcal{O}_z)$ holds for the original plant system (46). From the same discussion as that in Sec. IV-C together with the above results, we obtain the following no-go theorem:

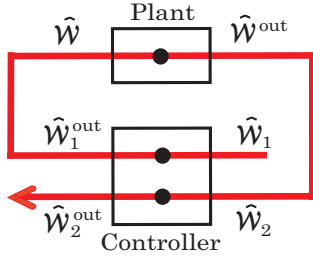


FIG. 7: A general configuration of the type-1 CF control.

Theorem 5: If the original plant system does not have a QND variable, then, any type-2 MF control cannot generate a QND variable in the closed-loop system.

D. DFS

Let us assume that the closed-loop system (43) with the output fields \hat{W}_1^{out} and \hat{W}_2^{out} , which now satisfy

$$\begin{bmatrix} \hat{W}_1^{\text{out}} \\ \hat{W}_2^{\text{out}} \end{bmatrix} = \begin{bmatrix} C_1 & C_{K1} \\ C_2 & C_{K2} \end{bmatrix} \begin{bmatrix} \hat{x} \\ x_K \end{bmatrix} + \begin{bmatrix} \hat{W}_1 \\ \hat{W}_2 \end{bmatrix},$$

contains a DFS. Equivalently, it contains a subsystem that is uncontrollable w.r.t. \hat{W}_1 and \hat{W}_2 and unobservable w.r.t. \hat{W}_1^{out} and \hat{W}_2^{out} . As before, a variable contained in the DFS is of the form $\hat{r} = v^\top \hat{x} = \tilde{v}^\top \hat{x}_e$. Then, first, the uncontrollability condition leads to the same results as in the QND case, i.e. $v \in \text{Ker}(\mathcal{C}_{\hat{W}_1}^\top) \cap \text{Ker}(\mathcal{C}_{\hat{W}_2}^\top)$ holds for the original plant system (46). Further, it is immediate to see that the unobservability condition yields $C_1 A^k v = 0$ and $C_2 A^k v = 0$ for all $k \geq 0$. Consequently, $v \in \text{Ker}(\mathcal{C}_{\hat{W}_1}^\top) \cap \text{Ker}(\mathcal{C}_{\hat{W}_2}^\top)$ and $v \in \text{Ker}(\mathcal{O}_{\hat{W}_1^{\text{out}}}) \cap \text{Ker}(\mathcal{O}_{\hat{W}_2^{\text{out}}})$ hold for the original plant system. Thus we have the following result.

Theorem 6: If the original plant system does not have a DFS, then, any type-2 MF control cannot generate a DFS in the closed-loop system.

VI. COHERENT FEEDBACK REALIZATIONS: TYPE-1 CASE

Here we turn our attention to the CF control and in what follows will see that, as shown in Table I, it has a capability of achieving the control goals, BAE, QND, and DFS. That is, as mentioned in Sec. I, these are situations where a quantum device has a clear advantage over a classical one. This section is devoted to prove the results in the type-1 CF case.

A. The closed-loop system with type-1 CF

The plant system is given by Eqs. (12) and (14) with input \hat{W} and output \hat{W}^{out} . In the type-1 control con-

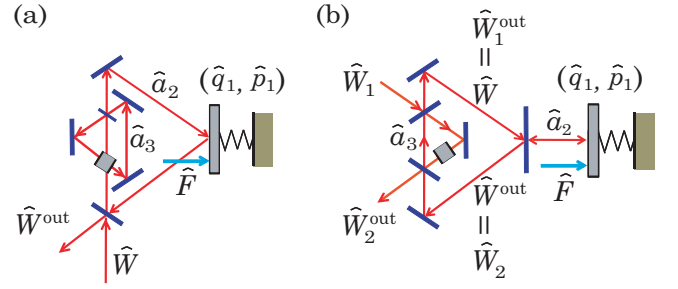


FIG. 8: (a) Direct interaction scheme achieving BAE for the opto-mechanical oscillator, proposed by Tsang and Caves [52]. (b) Equivalent realization via the type-1 CF control.

figuration, as described in Sec. IV, at most all the components of \hat{W}^{out} can be used for feedback, and also at most all the components of \hat{W} can be controlled. A CF controller is constructed by directly connecting another fully quantum system to the plant system by a feedback way. This means that, in the type-1 CF case, \hat{W}^{out} is connected to the controller's input and the controller's output is connected to \hat{W} , without involving any measurement process. The CF control configuration satisfying this setting, which avoids self-interaction of the fields, is depicted in Fig. 7. The controller has two kinds of input-output fields, and its system equation is given by

$$\begin{aligned} \frac{d\hat{x}_K}{dt} &= A_K \hat{x}_K + \Sigma C_1^\top \Sigma \hat{W}_1 + \Sigma C_2^\top \Sigma \hat{W}_2, \\ \hat{W}_1^{\text{out}} &= C_1 \hat{x}_K + \hat{W}_1, \quad \hat{W}_2^{\text{out}} = C_2 \hat{x}_K + \hat{W}_2, \end{aligned} \quad (48)$$

where $A_K = \Sigma(G_K + C_1^\top \Sigma C_1/2 + C_2^\top \Sigma C_2/2)$. The CF control is constructed by

$$\hat{W}_2 = \hat{W}^{\text{out}}, \quad \hat{W} = \hat{W}_1^{\text{out}}. \quad (49)$$

This condition imposes the size of C_1 and C_2 to be equal, although they are not necessarily of full rank. Note that more generally a scattering process from e.g. \hat{W}^{out} to \hat{W}_2 can be introduced, but here it is not necessary. Combining Eqs. (12), (14), (48), and (49), we obtain the dynamical equation of the closed-loop system:

$$\frac{d\hat{x}_e}{dt} = A_e \hat{x}_e + \Sigma C_e^\top \Sigma \hat{W}_1, \quad \hat{W}_2^{\text{out}} = C_e \hat{x}_e + \hat{W}_1, \quad (50)$$

where $\hat{x}_e = [\hat{x}^\top, \hat{x}_K^\top]^\top$, $A_e = \Sigma(G_e + C_e^\top \Sigma C_e/2)$, $C_e = [C, C_1 + C_2]$, and

$$G_e = \begin{bmatrix} G & C^\top \Sigma C_1/2 - C^\top \Sigma C_2/2 \\ \star & G_K + C_1^\top \Sigma^\top C_2/2 + C_2^\top \Sigma C_1/2 \end{bmatrix}.$$

\star denotes the symmetric elements of G_e .

B. BAE

Let us assume that we can engineer a CF controller satisfying $C_1 + C_2 = 0$. Then the closed-loop system

(50) takes the following form:

$$\begin{aligned} \frac{d\hat{x}_e}{dt} &= \begin{bmatrix} A & \Sigma C^\top \Sigma C_1 \\ \Sigma C_1^\top \Sigma^\top C & \Sigma G_K \end{bmatrix} \hat{x}_e + \begin{bmatrix} \Sigma C^\top \Sigma \\ 0 \end{bmatrix} \hat{W}_1, \\ \hat{W}_2^{\text{out}} &= [C, 0] \hat{x}_e + \hat{W}_1. \end{aligned} \quad (51)$$

The structure of this equation shows that, notably, the controller is directly coupled to the plant, yet there is no direct interaction between the field and the controller. This system configuration is called the *direct interaction*, meaning that an additional quantum device is prepared and is directly coupled to the plant system, not through input/output fields; hence the system (51) is a CF-based realization of the direct interaction.

Here we study the opto-mechanical oscillator described in Sec. II-C (ii), as a plant system. Since this system has one input-output field, the control configuration must be of type-1. Also it is easy to verify that this system does not satisfy BAE, and further, it does not have a QND variable. The goal is to design a CF controller such that BAE is realized for the closed-loop system toward high-precision detection of the unknown force \hat{F} . For this purpose, we take the CF scheme described above, leading to Eq. (51). The controller is single mode with variable $\hat{x}_K = [\hat{q}_3, \hat{p}_3]^\top$, and it has two input fields $\hat{W}_1 = [\hat{Q}_1, \hat{P}_1]^\top$ and $\hat{W}_2 = [\hat{Q}_2, \hat{P}_2]^\top$. The controller's system matrices are chosen so that they satisfy

$$\Sigma C_1^\top \Sigma^\top C = \begin{bmatrix} 0 & 0 \\ 0 & g \end{bmatrix}, \quad \Sigma G_K = \begin{bmatrix} -\omega & 0 \\ \omega & -\omega \end{bmatrix},$$

which leads to

$$C_1 = -C_2 = \frac{g}{\sqrt{2\gamma}} \begin{bmatrix} 0 & 0 \\ 1 & 0 \end{bmatrix}, \quad G_K = \begin{bmatrix} -\omega & 0 \\ 0 & -\omega \end{bmatrix}. \quad (52)$$

Physical implementation of the controller specified by these matrices will be discussed in the end of this subsection. Together with the term \hat{F} , which directly acts on \hat{p}_1 , the dynamics of the closed-loop system is given by

$$\frac{d\hat{x}_e}{dt} = A_e \hat{x}_e + B_e \hat{W}_1 + b_f \hat{F}, \quad \hat{W}_2^{\text{out}} = C_e \hat{x}_e + \hat{W}_1, \quad (53)$$

where

$$\begin{aligned} A_e &= \left[\begin{array}{c|c|c} 1/m & 0 & \\ \hline -m\omega^2 & \kappa & \\ \hline 0 & -\gamma & 0 \\ \hline \kappa & -\gamma & g \\ \hline & 0 & -\omega \\ & g & \omega \end{array} \right], \quad B_e = C_e^\top, \\ C_e &= \sqrt{2\gamma} \left[\begin{array}{c|c} 0 & 1 \\ \hline 0 & 1 \end{array} \right] \begin{bmatrix} 0 & 0 \\ 1 & 0 \end{bmatrix}, \quad b_f = [0, 1, 0, 0, 0, 0]^\top. \end{aligned}$$

Since \hat{Q}_2^{out} does not contain any information about \hat{F} , we need to measure \hat{P}_2^{out} , implying that the output signal is given by $y = M \hat{W}_2^{\text{out}} = \hat{P}_2^{\text{out}}$ with $M = [0, 1]$, i.e.

$$y = c_y \hat{x}_e + \hat{P}_1 = \sqrt{2\gamma} [0, 0, 0, 1, 0, 0] \hat{x}_e + \hat{P}_1. \quad (54)$$

The set of equations (53) and (54) is exactly the same as that of the modified opto-mechanical oscillator proposed by Tsang and Caves [52], which is shown in Fig. 8 (a). Notably, this system realizes BAE measurement for detecting \hat{F} ; in fact, with the choice $g = \kappa/\sqrt{m\omega}$ the transfer function from the BA noise \hat{Q}_1 to the output $y = \hat{P}_2^{\text{out}}$ takes zero:

$$y[s] = \frac{\sqrt{2\gamma}\kappa/m}{(s+\gamma)(s^2+\omega^2)} \hat{P}_1[s] + \frac{s-\gamma}{s+\gamma} \hat{F}[s].$$

Thus by injecting a \hat{P}_1 -squeezed light field (i.e. by reducing the noise of \hat{P}_1), in principle we can detect \hat{F} with better accuracy compared to the case without BAE. A detailed investigation of this BAE scheme in a practical setting was recently reported in [76].

Recall now that the system (53) and (54) is constructed by a CF control. That is, in a constructive way, we have proven that the type-1 CF control can realize BAE.

Lastly, let us consider an optical implementation of the above CF controller. The form of C_1 (or C_2) in Eq. (52) represents the so-called QND interaction of the controller and the field \hat{W}_1 (or \hat{W}_2), which can be physically implemented though in a nontrivial way [77]. The controller's Hamiltonian specified by G_K in Eq. (52) simply expresses the optical phase shift. Consequently, a detuned optical cavity coupled to two input-output fields via QND interactions, illustrated in Fig. 8 (b), is one possible physical realization of the CF controller proposed here. Note that its practical implementation is harder than that of the system given in [52]. But apart from such difficulty, again, what should be emphasized here is the fact that the type-1 CF control is capable of realizing BAE.

C. QND

Let us continue to examine the above CF-controlled opto-mechanical oscillator (53) and (54); actually we here show that this system contains QND variables, by proving Eq. (28), which is now $\text{Ker}(C_{\hat{W}_1}^\top) \cap \text{Range}(\mathcal{O}_y^\top) \neq \emptyset$.

First, if $g = \kappa/\sqrt{m\omega}$, the range of the controllability matrix $\mathcal{C}_{\hat{W}_1} = [B_e, A_e B_e, A_e^2 B_e]$ is spanned by the following independent vectors:

$$\begin{bmatrix} 0 \\ 0 \\ 1 \\ 0 \\ 0 \\ 0 \end{bmatrix}, \quad \begin{bmatrix} 0 \\ 0 \\ 1 \\ 0 \\ 0 \\ 0 \end{bmatrix}, \quad \begin{bmatrix} 0 \\ \kappa \\ 0 \\ 0 \\ 0 \\ g \end{bmatrix}, \quad \begin{bmatrix} \kappa/m \\ 0 \\ 0 \\ 0 \\ -g\omega \\ 0 \end{bmatrix}.$$

Note that $A_e^k B_e$ ($k \geq 3$) does not anymore produce an independent vector. Clearly,

$$v_1 = [0, -g, 0, 0, 0, \kappa]^\top, \quad v_2 = [g\omega, 0, 0, 0, \kappa/m, 0]^\top$$

are contained in $\text{Ker}(\mathcal{C}_{\hat{W}_1}^\top)$. Next, the kernel of the observability matrix $\mathcal{O}_y = [c_y^\top, A_e^\top c_y^\top, \dots]^\top$ is spanned by

$$\begin{bmatrix} 0 \\ 0 \\ 1 \\ 0 \\ 0 \\ 0 \end{bmatrix}, \begin{bmatrix} 0 \\ g\omega \\ 0 \\ 0 \\ 0 \\ \kappa/m \end{bmatrix}, \begin{bmatrix} -g \\ 0 \\ 0 \\ 0 \\ \kappa \\ 0 \end{bmatrix}.$$

But they are orthogonal to both v_1 and v_2 , meaning that v_1 and v_2 are contained in $\text{Range}(\mathcal{O}_y^\top)$. Consequently, we find that $v_1, v_2 \in \text{Ker}(\mathcal{C}_{\hat{W}_1}^\top) \cap \text{Range}(\mathcal{O}_y^\top)$. Thus

$$\hat{q}' = v_1^\top \hat{x}_e = -g\hat{p}_1 + \kappa\hat{p}_3, \quad \hat{p}' = v_2^\top \hat{x}_e = g\omega\hat{q}_1 + \frac{\kappa}{m}\hat{q}_3$$

are uncontrollable w.r.t. \hat{W}_1 and observable w.r.t. y (see the discussion around Eq. (28)); that is, \hat{q}' and \hat{p}' are QND variables generated by the CF control. Indeed, they are subjected to the dynamical equation of the form

$$\frac{d\hat{q}'}{dt} = \frac{\omega}{m}(g^2 m^2 \omega^2 + \kappa^2)\hat{p}', \quad \frac{d\hat{p}'}{dt} = -\frac{\omega}{m}(g^2 + \kappa^2)\hat{q}' + \hat{F}, \quad (55)$$

which clearly shows that (\hat{q}', \hat{p}') are free from \hat{W}_1 .

Here an interesting by-product is obtained. It is easy to see $[\hat{q}'(t), \hat{p}'(t)] = 0, \forall t$. Together with the fact that (\hat{q}', \hat{p}') are independent from other variables, this means that they are essentially classical variables which are detectable from the output field. In general, if a quantum system contains a subsystem whose variables are all commutative, then it is called a *classical subsystem* [72]; thus we now found that the CF-controlled opto-mechanical system (53) contains a classical subsystem (55).

D. DFS

To show that the type-1 CF control has capability of generating a DFS, let us return to the general closed-loop system (50). Suppose now that the original plant system (12) and (14) does not have a DFS, and further that a quantum controller with parameters $C_1 = C_2 = C/2$ and $G_K = G$ can be engineered. Hence, the plant and the controller have the same number of modes. Then Eq. (50) takes the following form:

$$\begin{aligned} \frac{d\hat{x}_e}{dt} &= A_e \hat{x}_e + B_e \hat{W}_1, \quad \hat{W}_2^{\text{out}} = C_e \hat{x}_e + \hat{W}_1, \\ A_e &= \begin{bmatrix} A & \Sigma C^\top \Sigma C/2 \\ \Sigma C^\top \Sigma C/2 & A \end{bmatrix}, \quad B_e = \begin{bmatrix} \Sigma C^\top \Sigma \\ \Sigma C^\top \Sigma \end{bmatrix}, \\ C_e &= [C, C]. \end{aligned} \quad (56)$$

Now we prove that this system contains a DFS, i.e. a subsystem that is uncontrollable w.r.t. \hat{W}_1 and unobservable w.r.t. \hat{W}_2^{out} . First, for the vector $v_e = [v^\top, -v^\top]^\top$ with v an arbitrary $2n$ -dimensional real vector, we have

$$v_e^\top A_e^k B_e = [v^\top (\Sigma G)^k, -v^\top (\Sigma G)^k] \begin{bmatrix} \Sigma C^\top \Sigma \\ \Sigma C^\top \Sigma \end{bmatrix} = 0,$$

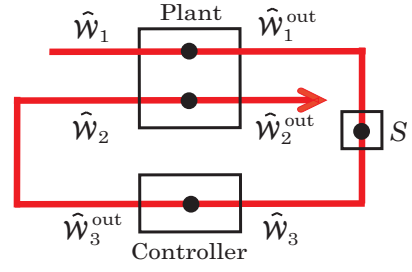


FIG. 9: A general configuration of the type-2 CF control.

for all $k \geq 0$. Hence, $v_e \in \text{Ker}(\mathcal{C}_{\hat{W}_1}^\top)$ holds with $\mathcal{C}_{\hat{W}_1} = [B_e, A_e B_e, A_e^2 B_e, \dots]$ the controllability matrix. Also,

$$C_e A_e^k v_e = [C, C] \begin{bmatrix} (\Sigma G)^k v \\ -(\Sigma G)^k v \end{bmatrix} = 0, \quad \forall k \geq 0$$

holds, implying $v_e \in \text{Ker}(\mathcal{O}_{\hat{W}_2^{\text{out}}})$ with $\mathcal{O}_{\hat{W}_2^{\text{out}}}$ the observability matrix $\mathcal{O}_{\hat{W}_2^{\text{out}}} = [C_e^\top, A_e^\top C_e^\top, \dots]^\top$. Consequently, v_e satisfies $v_e \in \text{Ker}(\mathcal{C}_{\hat{W}_1}^\top) \cap \text{Ker}(\mathcal{O}_{\hat{W}_2^{\text{out}}})$. This means, as discussed above Eq. (33), that $v_e^\top \hat{x}_e = v^\top \hat{x} - v^\top \hat{x}_K$ is uncontrollable and unobservable, hence this is the variable of a DFS generated by the CF control. Note that $2n$ independent vectors (v_1, \dots, v_{2n}) can be taken to construct $v_e^{(i)} = [v_i^\top, -v_i^\top]^\top$. Thus this DFS is composed of $2n$ variables $\{v_i^\top \hat{x} - v_i^\top \hat{x}_K\}_{i=1, \dots, 2n}$.

VII. COHERENT FEEDBACK REALIZATIONS: TYPE-2 CASE

In this section we study the type-2 CF control for realizing BAE, QND, and DFS. As in the type-1 case, a specific system achieving each control goal will be shown.

A. The closed-loop system with type-2 CF

As explained in Sec. V, the type-2 control means that two roles are given to the output fields of the plant system; one is for feedback control, and the other one is for evaluation. Hence the system to be controlled is

$$\begin{aligned} \frac{d\hat{x}}{dt} &= A\hat{x} + \Sigma C_1^\top \Sigma \hat{W}_1 + \Sigma C_2^\top \Sigma \hat{W}_2, \\ \hat{W}_1^{\text{out}} &= C_1 \hat{x} + \hat{W}_1, \quad \hat{W}_2^{\text{out}} = C_2 \hat{x} + \hat{W}_2. \end{aligned} \quad (57)$$

For designing a CF controller, there are some variation in its structure. Here we particularly consider the CF control configuration illustrated in Fig. 9; that is, the controller has a single kind of input-output fields that are directly connected to the plant's input and output fields. For a general type-2 CF control configuration, see [22]. Note also that, in our case, C_1 and C_2 are of the same size, although they are not necessarily of full rank.

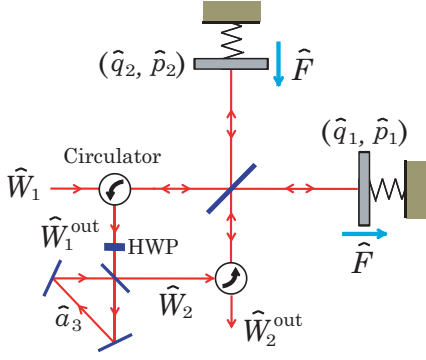


FIG. 10: Michelson's interferometer with type-2 CF. The CF controller is an optical cavity with coupling constant ϵ and detuning α . HWP: half wave plate.

Hence the dynamics of the CF controller is given by

$$\frac{d\hat{x}_K}{dt} = A_K \hat{x}_K + \Sigma C_K^\top \Sigma \hat{W}_3, \quad \hat{W}_3^{\text{out}} = C_K \hat{x}_K + \hat{W}_3,$$

where $A_K = \Sigma(G_K + C_K^\top \Sigma C_K/2)$, and the feedback connection is realized by

$$\hat{W}_3 = S \hat{W}_1^{\text{out}}, \quad \hat{W}_2 = \hat{W}_3^{\text{out}}.$$

Here S is an orthogonal and symplectic matrix representing a scattering process from \hat{W}_1^{out} to \hat{W}_3 . Combining the above equations yields the dynamical equation of the closed-loop system;

$$\frac{d\hat{x}_e}{dt} = A_e \hat{x}_e + \Sigma C_e^\top \Sigma S \hat{W}_1, \quad \hat{W}_2^{\text{out}} = C_e \hat{x}_e + S \hat{W}_1, \quad (58)$$

where $\hat{x}_e = [\hat{x}^\top, \hat{x}_K^\top]^\top$ and

$$A_e = \Sigma[G_e + C_e^\top \Sigma C_e/2], \quad C_e = [SC_1 + C_2, C_K],$$

$$G_e = \begin{bmatrix} G + (C_2^\top \Sigma SC_1 + C_1^\top S^\top \Sigma^\top C_2)/2 & \star \\ C_K^\top \Sigma(SC_1 - C_2)/2 & G_K \end{bmatrix}.$$

\star denotes the symmetric elements of G_e .

B. BAE

To demonstrate that the type-2 CF is capable of realizing BAE, we here study the Michelson's interferometer as a plant system, which is described in Sec. II-C (iii) with Fig. 3 (c). The system is composed of two oscillators driven by an unknown force \hat{F} along opposite directions. The oscillators' dynamical motion is described by Eq. (19), which is specified by the following system matrices: $G = \text{diag}\{m\omega^2, 1/m, m\omega^2, 1/m\}$ and

$$C_1 = \sqrt{\lambda} \begin{bmatrix} 0 & 0 \\ 1 & 1 \end{bmatrix}, \quad C_2 = \sqrt{\lambda} \begin{bmatrix} 0 & 0 \\ 1 & -1 \end{bmatrix}.$$

This system works as a sensor for detecting the force \hat{F} ; but as explained before, the noise power of the output

signal is bounded from below by the SQL (21). Hence the purpose here is to design a CF controller that realizes BAE and as a result beats the SQL. Actually, the plant system has two input-output ports, hence it can be treated within the type-2 CF control framework.

Here we consider the CF configuration described in the previous subsection. That is, \hat{W}_1^{out} and \hat{W}_2 are optically connected through CF. In particular, as a CF controller, let us take a single input-output optical cavity, whose dynamical equation is specified by the following matrices:

$$G_K = \begin{bmatrix} \alpha & 0 \\ 0 & \beta \end{bmatrix}, \quad C_K = \sqrt{2\epsilon} \begin{bmatrix} 1 & 0 \\ 0 & 1 \end{bmatrix}, \quad S = \begin{bmatrix} 0 & 1 \\ -1 & 0 \end{bmatrix},$$

where ϵ is the coupling constant between the field and the cavity mode. Later we will set $\alpha = \beta$, which thus represents the detuning. S represents a phase shift acting on the input optical field in the form $\hat{A}_3 = -i\hat{A}_1^{\text{out}}$. Thus the closed-loop system is a 3-modes single input-output linear system, depicted in Fig. 10.

With the above setup, the closed-loop system (58) takes the following form:

$$\frac{d\hat{x}_e}{dt} = A_e \hat{x}_e + B_e \hat{W}_1' + b_f \hat{F}, \quad \hat{W}_2^{\text{out}} = C_e \hat{x}_e + \hat{W}_1',$$

$$A_e = \begin{bmatrix} \lambda - m\omega^2 & 1/m & 0 \\ 0 & \lambda & \sqrt{2\lambda\epsilon} \\ -\lambda & -\lambda - m\omega^2 & 0 \\ -\sqrt{2\lambda\epsilon} & -\sqrt{2\lambda\epsilon} & -\epsilon & \beta \\ 0 & 0 & -\alpha & -\epsilon \end{bmatrix},$$

$$B_e = \Sigma C_e^\top \Sigma = [b_1, b_2] = \begin{bmatrix} 0 & 0 \\ \sqrt{\lambda} & -\sqrt{\lambda} \\ 0 & 0 \\ -\sqrt{\lambda} & -\sqrt{\lambda} \\ -\sqrt{2\epsilon} & 0 \\ 0 & -\sqrt{2\epsilon} \end{bmatrix},$$

$$b_f = [0 \ 1 \ 0 \ -1 \ 0 \ 0]^\top,$$

$$C_e = \begin{bmatrix} c_1^\top \\ c_2^\top \end{bmatrix} = \begin{bmatrix} \sqrt{\lambda} & 0 & \sqrt{\lambda} & 0 \\ \sqrt{\lambda} & 0 & -\sqrt{\lambda} & 0 \end{bmatrix} \begin{bmatrix} \sqrt{2\epsilon} & 0 \\ 0 & \sqrt{2\epsilon} \end{bmatrix},$$

$$\hat{W}_1' = S \hat{W}_1 = [\hat{P}_1, -\hat{Q}_1]^\top. \quad (59)$$

Let us seek the parameters $(\alpha, \beta, \epsilon)$ that achieve BAE. First, it is easy to see $c_1^\top A_e^k b_f = 0, \forall k \geq 0$, or equivalently $\text{Ker}(C_F^\top)^c \cap \text{Range}(\mathcal{O}_{\hat{Q}_2^{\text{out}}}^\top) = \emptyset$; that is, \hat{Q}_2^{out} does not contain any information about \hat{F} . Thus we measure

$$y = \hat{P}_2^{\text{out}} = c_2^\top \hat{x}_e - \hat{Q}_1, \quad (60)$$

implying that \hat{Q}_1 is the shot noise while \hat{P}_1 is the BA noise. Thus the parameters should be chosen so that the BAE condition (24) i.e. $\text{Ker}(C_{\hat{P}_1}^\top)^c \cap \text{Range}(\mathcal{O}_y^\top) = \emptyset$ is satisfied, which is carried out by examining the equivalent condition (25): $c_2^\top A_e^k b_1 = 0, \forall k \geq 0$. The case $k = 0$ is

already satisfied. To see the case $k \geq 1$, let us focus on

$$A_e b_1 = \begin{bmatrix} \sqrt{\lambda}/m \\ 0 \\ -\sqrt{\lambda}/m \\ 0 \\ -\epsilon\sqrt{2\epsilon} \\ \alpha\sqrt{2\epsilon} \end{bmatrix}, \quad A_e^2 b_1 = \begin{bmatrix} 0 \\ -(\omega^2 + 2\epsilon^2)\sqrt{\lambda} \\ 0 \\ (\omega^2 + \epsilon^2/2)\sqrt{\lambda} \\ (\alpha\beta + \epsilon^2)\sqrt{2\epsilon} \\ 0 \end{bmatrix},$$

where the proportional part to b_1 are subtracted. Then, the condition is satisfied if we impose $c_2^\top A_e b_1 = 0$ and $A_e^2 b_1 \propto b_1$, which yield

$$\frac{\lambda}{m} + \alpha\epsilon = 0, \quad \omega^2 + 2\epsilon^2 = \alpha\beta + \epsilon^2.$$

Let us especially take the parameter $\alpha = \beta < 0$, implying that the CF controller is an optical cavity with negative detuning α . The parameters are then explicitly given by

$$\epsilon = \frac{\sqrt{2}\lambda}{m\sqrt{\omega^2 + \sqrt{\omega^4 + 4\lambda^2/m^2}}}, \quad \alpha = \frac{-\lambda}{m\epsilon}. \quad (61)$$

When $\omega \ll 1$, they are approximated by $\sqrt{\lambda/m}$ and $-\sqrt{\lambda/m}$, respectively. Actually under the condition (61), the output is described in the Laplace domain by

$$y[s] = -\frac{s^3 - \epsilon s^2 + \omega^2 s + \epsilon(\omega^2 + 2\epsilon^2)}{(s^2 + \omega^2)(s + \epsilon)} \hat{Q}_1[s] + \frac{2\sqrt{\lambda}}{m(s^2 + \omega^2)} \hat{F}[s],$$

which is free from the BA noise $\hat{P}_1[s]$. As expected, this BAE measurement beats the SQL and enables high-precision detection of \hat{F} . To see this fact, let us evaluate the power spectrum density of the noise. As seen before, \hat{F} induces the oscillators's position shift \hat{g} in the Fourier domain $s = i\Omega$ by $\hat{F}[i\Omega] = -mL\Omega^2 \hat{g}[i\Omega]$. Then, under the assumption $\omega \ll \Omega$, the normalized signal is given by

$$\tilde{y}[i\Omega] = \frac{y[i\Omega]}{2\sqrt{\lambda}L} = \hat{g}[i\Omega] - \frac{i\Omega^3 - \epsilon\Omega^2 - 2\epsilon^3}{2\sqrt{\lambda}L\Omega^2(i\Omega + \epsilon)} \hat{Q}_1[i\Omega].$$

Using $\epsilon = \sqrt{\lambda/m}$ we obtain

$$S[i\Omega] = \langle |\tilde{y} - \hat{g}|^2 \rangle = \left(\frac{\lambda}{m^2 L^2 \Omega^4} + \frac{1}{4\lambda L^2} \right) \langle |\hat{Q}_1|^2 \rangle,$$

which has the same form as that of the non-controlled scheme in Eq. (21), except that the BA noise is replaced by the shot noise. Therefore, by injecting a \hat{Q}_1 -squeezed light field into the *first* input port (i.e. the bright port), we can realize a broadband noise reduction below the SQL (21) in the output noise power. It should be noted again that, without squeezing of the input field, the output noise power of the CF-controlled interferometer having the BAE property reproduces the SQL. This means that achieving BAE itself does not necessarily result in

the increased force sensitivity; in fact we need to combine the BAE property and squeezing of the input.

Note that, while we have found a CF controller achieving BAE for high-precision detection of \hat{F} below the SQL, the result obtained here does not mean to emphasize that the proposed schematic is an alternative configuration for gravitational wave detection. Actually, the schematic is very different from several effective methods, particularly in that the second output port is not anymore a dark port. Hence the amplitude component must be subtracted from the output field, which though cannot be carried out perfectly; thus the above-described ideal detection of \hat{g} below the SQL would be a difficult task in a practical situation. Rather the main purpose here is to prove the capability of a type-2 CF controller for realizing BAE. Also, as demonstrated above, it is remarkable that the problem for designing BAE can be solved, by a system theoretic approach based on the controllability/observability notion; this approach might shed a new light on the engineering problems for gravitational wave detection.

C. QND

We here see that the closed-loop system studied in the previous subsection contains QND variables. Note that the original interferometer does not have a QND variable.

First let us calculate the controllability matrix $\mathcal{C}_{\hat{W}'_1} = [B_e, A_e B_e, A_e^2 B_e, \dots]$ with A_e and B_e given in Eq. (59). It was already seen that b_1 generates two dimensional subspace spanned by b_1 and $A_e b_1$, under the condition (61). Now, by further imposing $\alpha = \beta$, we have $A_e^2 b_2 = -\omega^2 b_2$, implying that $\text{Range}(\mathcal{C}_{\hat{W}'_1})$ is spanned by

$$\begin{bmatrix} 0 \\ \sqrt{\lambda} \\ 0 \\ -\sqrt{\lambda} \\ -\sqrt{2\epsilon} \\ 0 \end{bmatrix}, \quad \begin{bmatrix} 0 \\ \sqrt{\lambda} \\ 0 \\ \sqrt{\lambda} \\ 0 \\ \sqrt{2\epsilon} \end{bmatrix}, \quad \begin{bmatrix} \sqrt{\lambda}/m \\ 0 \\ -\sqrt{\lambda}/m \\ 0 \\ -\epsilon\sqrt{2\epsilon} \\ \alpha\sqrt{2\epsilon} \end{bmatrix}, \quad \begin{bmatrix} \sqrt{\lambda}/m \\ 0 \\ \sqrt{\lambda}/m \\ 0 \\ \beta\sqrt{2\epsilon} \\ -\epsilon\sqrt{2\epsilon} \end{bmatrix}.$$

Hence $\dim \text{Range}(\mathcal{C}_{\hat{W}'_1}) = 4$. Let us take two independent vectors v_1 and v_2 spanning $\text{Ker}(\mathcal{C}_{\hat{W}'_1}^\top)$; then $v_1^\top \hat{x}_e$ and $v_2^\top \hat{x}_e$ are not affected by the input field \hat{W}'_1 . Moreover, these variables appear in the output signal (60) as shown below. Actually we can prove that c_2 and $A_e^\top c_2$ are both independent to the above four vectors, implying

$$\text{Range}(\mathcal{C}_{\hat{W}'_1}) \oplus \text{span}\{c_2, A_e^\top c_2\} = \mathbb{R}^6.$$

Thus $\text{Range}(\mathcal{C}_{\hat{W}'_1}) \cup \text{Range}(\mathcal{O}_y^\top) = \mathbb{R}^6$ holds, which further leads to $\text{Range}(\mathcal{C}_{\hat{W}'_1})^c \subseteq \text{Range}(\mathcal{O}_y^\top)$. Consequently, we find $v_1, v_2 \in \text{Range}(\mathcal{O}_y^\top)$, meaning that $v_1^\top \hat{x}_e$ and $v_2^\top \hat{x}_e$ appear in y and thus they are QND variables. That is, the type-2 CF controller described in Sec. VII-B has capability of generating QND variables.

D. DFS

Lastly we again study a general CF-controlled system (58); suppose that the plant system (57) satisfies $C_1 = C_2 = C/2$ and does not contain a DFS. Further, let us choose a type-2 CF controller with system matrices $G_K = G$ and $C_K = C$, which is directly connected to the plant (i.e. $S = I$). Then Eq. (58) takes exactly the same form as Eq. (56), which contains a DFS. Therefore, this type-2 CF controller has ability to generate a DFS.

VIII. CONCLUSION AND FUTURE WORKS

This paper has given some general answers to the question about whether or not measurement should be involved in the feedback structure for controlling a quantum system. That is, for a general linear quantum system, we have obtained the no-go theorems stating that the control goal, realization of BAE, QND, or DFS, cannot be achieved by any MF control; on the other hand, for each control goal, we have found an example of CF control accomplishing the task. From the viewpoint that MF is essentially a classical operation on the system while CF is a fully quantum one, these results imply that BAE, QND, and DFS are genuine quantum objectives that cannot be realized by any feedback-based classical operation.

The key idea to obtain all the results is the following system theoretic characterizations of BAE, QND, and DFS, which are also summarized in Fig. 2:

$$\text{BAE: } \text{Ker}(\mathcal{C}_{\hat{\mathcal{P}}}^\top)^c \cap \text{Range}(\mathcal{O}_y^\top) = \emptyset,$$

$$\text{QND: } \text{Ker}(\mathcal{C}_{\hat{\mathcal{W}}}^\top) \cap \text{Range}(\mathcal{O}_y^\top) \neq \emptyset,$$

$$\text{DFS: } \text{Ker}(\mathcal{C}_{\hat{\mathcal{W}}}^\top) \cap \text{Range}(\mathcal{O}_{\hat{\mathcal{W}}_{\text{out}}}^\top)^c \neq \emptyset.$$

Now we should remember the following equivalent characterizations in terms of transfer functions:

$$\text{BAE: } \Xi_{\hat{\mathcal{P}} \rightarrow y}[s] = 0, \forall s,$$

$$\text{QND: } \Xi_{\hat{\mathcal{W}} \rightarrow \hat{x}_2'}[s] = 0, \forall s \text{ \& } \Xi_{\hat{x}_2' \rightarrow y}[s] \neq 0, \exists s,$$

$$\text{DFS: } \Xi_{\hat{\mathcal{W}} \rightarrow \hat{x}_2'}[s] = 0, \forall s \text{ \& } \Xi_{\hat{x}_2' \rightarrow \hat{\mathcal{W}}_{\text{out}}}[s] = 0, \forall s.$$

Although in this paper these characterizations are not fully used except Sec. V-B, they will serve as powerful tools in quantum device engineering in a practical situation. In fact, in reality due to several experimental imperfections, it is often the case that the controllability/observability matrix becomes of full rank, and thus the perfect achievement of the above geometric conditions cannot be expected. Nonetheless, the functional approach based on the transfer function allows us to obtain an approximate solution of those problems. For instance for the BAE case, even if $\text{Ker}(\mathcal{C}_{\hat{\mathcal{P}}}^\top)^c \cap \text{Range}(\mathcal{O}_y^\top) = \emptyset$ or equivalently $\Xi_{\hat{\mathcal{P}} \rightarrow y}[s] = 0, \forall s$ is never satisfied, an approximate BAE measurement can be engineered by solving a minimization problem $\|\Xi_{\hat{\mathcal{P}} \rightarrow y}[s]\| \rightarrow \min$. Actually, in the history of classical control, the so-called geometric

control theory was first deeply investigated [8], pursuing e.g. ideal disturbance decoupling. Later, towards wider applicability of the control theory, several functional approaches were developed [9]; the linear quadratic Gaussian (LQG) control and H^∞ control, which are respectively based on the minimization of the H^2 norm $\|\cdot\|_2$ and the H^∞ norm $\|\cdot\|_\infty$ of a transfer function, are typical successful results. A notable fact is that, as mentioned in Sec. I, recently quantum versions of those classical feedback control methods have been deeply developed. Therefore combination of the geometric and functional approaches will constitute a new methodology in the field of quantum control and information. Of course, under the evaluation of minimizing a norm of a transfer function, comparing MF and CF controls again becomes an open problem.

Another important direction of the future research is to extend the results to the nonlinear case. Actually the control goals, BAE, QND, DFS, are all essential as well in nonlinear systems, such as optical devices with high order nonlinearity, photonic crystal arrays, and coupled qubits networks. The strength of the input-output formalism [36, 37] is in that it is applicable to a very wide class of such Markovian nonlinear systems. More precisely, for a general system that couples with m probe/environment fields, its variable $\hat{X}(t)$ is governed by the following quantum stochastic differential equation:

$$\begin{aligned} \frac{d\hat{X}}{dt} = & i[\hat{H}, \hat{X}] + \sum_{j=1}^m (\hat{L}_j^* \hat{X} \hat{L}_j - \frac{1}{2} \hat{L}_j^* \hat{L}_j \hat{X} - \frac{1}{2} \hat{X} \hat{L}_j^* \hat{L}_j) \\ & + \sum_{j=1}^m ([\hat{X}, \hat{L}_j] \hat{A}_j^* - [\hat{X}, \hat{L}_j^*] \hat{A}_j), \end{aligned} \quad (62)$$

where \hat{H} is the system Hamiltonian and \hat{L}_j is the coupling operator. Also the j th output field satisfies

$$\hat{A}_j^{\text{out}} = \hat{L}_j + \hat{A}_j. \quad (63)$$

In fact, the nonlinear atomic ensemble dynamics (27) is obtained by setting $\hat{H} = 0$ and $\hat{L} = \sqrt{M} \hat{J}_z$ in Eq. (62). (Also, the linear system (12) and (14) corresponds to the case $\hat{H} = \hat{x}^\top G \hat{x}/2$ and $\hat{L}_j = c_j^\top \hat{x}$.) Very importantly, there exists a celebrated classical nonlinear systems and control theory [78, 79], that gives clear characterizations of controllability and observability notions even for nonlinear systems. Therefore it is expected that, by taking a similar approach shown in this paper, we can have a unified formalism of BAE, QND, and DFS for a general quantum nonlinear system (62) and (63). This should be very useful for systematic engineering of wider class of quantum information processing devices; but, as in the case discussed in the previous paragraph, comparison of MF and CF for nonlinear systems is also a nontrivial task. An interesting result along this direction was recently reported in [80]; for the problem detecting a force driving a linear oscillator, a MF has clear advantage over the non-controlled system with an optimized estimator, only when the oscillator contains some nonlinearity.

Acknowledgments

This work was supported in part by JSPS Grant-in-Aid No. 40513289. The author acknowledges helpful discussions with I. R. Petersen.

Appendix A: Direct measurement feedback

In this paper, from the standpoint comparing CF and MF, we assumed that a MF controller is given by a *dynamical* one with internal variable x_K and that the control is carried out by modulating the plant's input fields. However, the control configuration is not limited to the dynamical one; the *direct (or proportional) measurement feedback* developed by Wiseman [81] is indeed the first proposal applying the classical feedback control in the quantum domain. As discussed in the literature (e.g. see [1]), an ideal MF control is actually effective in controlling the system; what is most notable here is the fact obtained in [46], clarifying that a direct MF can produce a QND variable, unlike the dynamical one. Let us here review this result.

The plant system is an optical cavity containing a χ^2 nonlinear crystal, and further, the cavity mode can be directly controlled by a modulator. The output signal is obtained by measuring the amplitude quadrature of the output field. The system equations are then given by

$$\frac{d\hat{x}}{dt} = \begin{bmatrix} -\kappa & 0 \\ 0 & 0 \end{bmatrix} \hat{x} + \begin{bmatrix} 1 \\ 0 \end{bmatrix} u - \sqrt{\kappa} \begin{bmatrix} \hat{Q} \\ \hat{P} \end{bmatrix}, \quad y = \sqrt{\kappa}\hat{q} + \hat{Q},$$

where $\hat{x} = [\hat{q}, \hat{p}]^T$ is the cavity mode quadratures, $u(t)$ is the control signal representing the amplitude modulation, and κ is the coupling strength between the cavity and the probe field. Note that this modulation effect does not appear in the output. The direct feedback considered in [46] is of the form $u = \sqrt{\kappa}y$, which enables us to modify the system dynamics so that \hat{x} evolves in time with the following linear equation:

$$\frac{d}{dt} \begin{bmatrix} \hat{q} \\ \hat{p} \end{bmatrix} = -\sqrt{\kappa} \begin{bmatrix} 0 \\ 1 \end{bmatrix} \hat{P}, \quad y = \sqrt{\kappa}\hat{q} + \hat{Q}.$$

Clearly, \hat{q} is not disturbed by the noise while it appears in the output signal, implying that we can measure \hat{q} without disturbing it. That is, \hat{q} is a QND variable.

The above result means that the type-1 no-go theorem for QND does not hold, if an ideal direct MF can be employed. However, we should note a critical assumption that an ideal direct MF controller has infinite bandwidth. Hence let us further examine a practical case where the feedback circuit has a finite bandwidth and its dynamics is given by

$$\frac{dx_K}{dt} = -\frac{1}{\tau}x_K + \frac{1}{\tau}y, \quad u = \sqrt{\kappa}x_K, \quad (\text{A1})$$

where τ represents the time constant and x_K is the internal variable of the circuit. Actually the transfer function from y to u is given by $\Xi_{y \rightarrow u}[s] = \sqrt{\kappa}/(1 + \tau s)$, whose gain in the Fourier domain is computed as

$$|\Xi_{y \rightarrow u}[i\Omega]|^2 = \frac{\kappa}{1 + \tau^2\Omega^2}.$$

The bandwidth is defined by $[-1/\tau, 1/\tau]$, in which more than half the power of the signal y is allowed to pass through the circuit. This clearly shows that the MF is only available in the infinite bandwidth limit $\tau \rightarrow +0$. We can also see the finite bandwidth effect on the ideal QND variable \hat{q} as follows; the combined system dynamics of the cavity and the circuit is given by

$$\frac{d}{dt} \begin{bmatrix} \hat{q} \\ x_K \end{bmatrix} = \begin{bmatrix} -\kappa & \sqrt{\kappa} \\ \sqrt{\kappa}/\tau & -1/\tau \end{bmatrix} \begin{bmatrix} \hat{q} \\ x_K \end{bmatrix} + \begin{bmatrix} -\sqrt{\kappa} \\ 1/\tau \end{bmatrix} \hat{Q},$$

which yields

$$\Xi_{\hat{Q} \rightarrow \hat{q}}[s] = \frac{-\sqrt{\kappa}\tau}{(\kappa\tau + 1) + \tau s}.$$

Thus, actually in the ideal limit $\tau \rightarrow +0$, the variable \hat{q} becomes QND. In other words, a practical direct MF does not generate a QND variable. Note that controlling via the field modulation $\hat{Q} \rightarrow \hat{Q} + u$ together with the finite-bandwidth MF controller (A1) is exactly the type-I MF, meaning that the no-go theorem is applied to this practical case. We should rather have an understanding that the controller (A1) is an effective MF realizing an approximated QND variable in the scenario discussed in Sec. VIII.

-
- [1] H. M. Wiseman and G. J. Milburn, *Quantum Measurement and Control* (Cambridge University Press, 2010)
 - [2] A. Barchielli and M. Gregoratti, *Quantum Trajectories and Measurements in Continuous Time: The Diffusive Case*, Lect. Notes Phys. **782** (Springer, Berlin, 2009)
 - [3] L. Bouten, R. van Handel, and M. R. James, A discrete invitation to quantum filtering and feedback control, *SIAM Review* **51**, 239/316 (2009)

- [4] V. P. Belavkin, Quantum stochastic calculus and quantum nonlinear filtering, *J. Multivariate Anal.* **42**, 171 (1992)
- [5] V. P. Belavkin, Quantum diffusion, measurement and filtering I, *Theor. Probab. Appl.* **38**, 573 (1993)
- [6] L. Bouten, R. van Handel, and M. R. James, An introduction to quantum filtering, *SIAM J. Contr. Optim.* **46**-6, 2199/2241 (2007)

- [7] T. Kailath, *Linear Systems* (Englewood Cliffs, NJ: Prentice-Hall, 1980)
- [8] W. M. Wonham, *Linear Multivariable Control: A Geometric Approach*, 3rd ed. (Springer-Verlag, 1985)
- [9] K. Zhou and J. C. Doyle, *Essentials of Robust Control* (Prentice Hall, 1997)
- [10] A. C. Doherty and K. Jacobs, Feedback control of quantum systems using continuous state estimation, *Phys. Rev. A* **60**, 2700 (1999)
- [11] A. Hopkins, K. Jacobs, S. Habib, and K. Schwab, Feedback cooling of a nanomechanical resonator, *Phys. Rev. B* **68**, 235328 (2003)
- [12] R. Hamerly and H. Mabuchi, Advantages of coherent feedback for cooling quantum oscillators, *Phys. Rev. Lett.* **105**, 123601 (2013)
- [13] R. Hamerly and H. Mabuchi, Coherent controllers for optical-feedback cooling of quantum oscillators, *Phys. Rev. A* **87**, 013815 (2013)
- [14] C. Ahn, A. C. Doherty, and A. J. Landahl, Continuous quantum error correction via quantum feedback control, *Phys. Rev. A* **65**, 042301 (2002)
- [15] H. Mabuchi, Continuous quantum error correction as classical hybrid control, *New J. Phys.* **11**, 105044 (2009)
- [16] G. Tajimi and N. Yamamoto, Dynamical Gaussian state transfer with quantum error correction architecture, *Phys. Rev. A* **11**, 022303 (2012)
- [17] C. Sayrin, et. al., Real-time quantum feedback prepares and stabilizes photon number states, *Nature* **477**, 73 (2011)
- [18] R. Vijay, C. Macklin, D. H. Slichter, S. J. Weber, K. W. Murch, R. Naik, A. N. Korotkov, and I. Siddiqi, Stabilizing Rabi oscillations in a superconducting qubit using quantum feedback, *Nature* **490**, 77 (2012)
- [19] S. Shankar et. al., Autonomously stabilized entanglement between two superconducting quantum bits, *Nature* **504**, 419 (2013)
- [20] R. Inoue, S. Tanaka, R. Namiki, T. Sagawa, and Y. Takahashi, Unconditional quantum-noise suppression via measurement-based quantum feedback, *Phys. Rev. Lett.* **110**, 163602 (2013)
- [21] H. M. Wiseman and G. J. Milburn, All-optical versus electro-optical quantum-limited feedback, *Phys. Rev. A* **49**, 4110 (1994)
- [22] M. R. James, H. I. Nurdin, and I. R. Petersen, H^∞ control of linear quantum stochastic systems, *IEEE Trans. Automat. Contr.* **53**-8, 1787/1803 (2008)
- [23] J. E. Gough and M. R. James, The series product and its application to quantum feedforward and feedback networks, *IEEE Trans. Automat. Contr.* **54**-11, 2530/2544 (2009)
- [24] H. I. Nurdin, M. R. James, and A. C. Doherty, Network synthesis of linear dynamical quantum stochastic systems, *SIAM J. Control Optim.* **48**-4, 2686/2718 (2009)
- [25] J. E. Gough, M. R. James, and H. I. Nurdin, Squeezing components in linear quantum feedback networks, *Phys. Rev. A* **81**, 023804 (2010)
- [26] M. Yanagisawa and H. Kimura, Transfer function approach to quantum control— Part I: Dynamics of quantum feedback systems, *IEEE Trans. Automat. Contr.* **48**-12, 2107/2120 (2003)
- [27] J. E. Gough and S. Wildfeuer, Enhancement of field squeezing using coherent feedback, *Phys. Rev. A* **80**, 42107 (2009)
- [28] J. Kerckhoff, H. I. Nurdin, D. Pavlichin, and H. Mabuchi, Designing quantum memories with embedded control: Photonic circuits for autonomous quantum error correction, *Phys. Rev. Lett.* **105**, 040502 (2010)
- [29] H. Mabuchi, Coherent-feedback control strategy to suppress spontaneous switching in ultra-low power optical bistability, *Appl. Phys. Lett.* **98**, 193109 (2011)
- [30] H. Mabuchi, Coherent-feedback quantum control with a dynamic compensator, *Phys. Rev. A* **78**, 32323 (2008)
- [31] S. Iida, M. Yukawa, H. Yonezawa, N. Yamamoto, and A. Furusawa, Experimental demonstration of coherent feedback control on optical field squeezing, *IEEE Trans. Automat. Contr.* **57**-8, 2045/2050 (2012)
- [32] O. Crisafulli, N. Tezak, D. B. S. Soh, M. A. Armen, and H. Mabuchi, Squeezed light in an optical parametric oscillator network with coherent feedback quantum control, *Optics Express* **21**-15, 18372 (2013)
- [33] J. Kerckhoff et. al., Tunable coupling to a mechanical oscillator circuit using a coherent feedback network, *Phys. Rev. X* **3**, 021013 (2013)
- [34] H. I. Nurdin, M. R. James, and I. R. Petersen, Coherent quantum LQG control, *Automatica* **45**, 1837/1846 (2009)
- [35] K. Jacobs, X. Wang, and H. M. Wiseman, Coherent feedback that beats all measurement-based feedback protocols, *New J. Phys.* **16**, 073036 (2014)
- [36] C. W. Gardiner and P. Zoller, *Quantum Noise* (Berlin: Springer, 2000)
- [37] D. F. Walls and G. J. Milburn, *Quantum Optics*, 2nd ed. (Springer, 2008)
- [38] V. B. Braginsky and F. Y. Khalili, *Quantum Measurement* (Cambridge University Press, Cambridge; New York, 1992)
- [39] C. M. Caves, K. S. Thorne, R. W. P. Drever, V. D. Sandberg, and M. Zimmermann, On the measurement of a weak classical force coupled to a quantum-mechanical oscillator, I, Issues of principle, *Rev. Mod. Phys.* **52**, 341 (1980)
- [40] V. B. Braginsky, Y. I. Vorontsov, and K. S. Thorne, Quantum nondemolition measurements, *Science* **209**, 547 (1980).
- [41] P. Zanardi and M. Rasetti, Noiseless quantum codes, *Phys. Rev. Lett.* **79**, 3306 (1997)
- [42] D. A. Lidar and K. B. Whaley, Decoherence-free subspaces and subsystems, *Irreversible Quantum Dynamics*, ed. F. Benatti and R. Floreanini (Berlin: Springer) *Lect. Notes Phys.* **622**, 83 (2003)
- [43] J. M. Courty, A. Heidmann, and M. Pinard, Back-action cancellation in interferometers by quantum locking, *Europhys. Lett.* **63**-2, 226/232 (2003)
- [44] J. M. Courty, A. Heidmann, and M. Pinard, Quantum locking of mirrors in interferometers, *Phys. Rev. Lett.* **90**, 083601 (2003)
- [45] D. Vitali, M. Punturo, S. Mancini, P. Amico, and P. Tombesi, Noise reduction in gravitational wave interferometers using feedback, *J. Opt. B: Quantum Semiclass. Opt.* **6**, 691 (2004)
- [46] H. M. Wiseman, Using feedback to eliminate back-action in quantum measurements, *Phys. Rev. A* **51**, 2459 (1995)
- [47] F. Ticozzi and L. Viola, Quantum Markovian subsystems: Invariance, attractivity and control, *IEEE Trans. Automat. Contr.* **53**-9, 2048/2063 (2008)
- [48] F. Ticozzi and L. Viola, Analysis and synthesis of attractive quantum Markovian dynamics, *Automatica* **45**-9, 2002/2009 (2009)

- [49] S. G. Schirmer and X. Wang, Stabilizing open quantum systems by Markovian reservoir engineering, *Phys. Rev. A* **81**, 062306 (2010)
- [50] H. A. Bachor and T. C. Ralph, *A Guide to Experiments in Quantum Optics* (Weinheim, Wiley-VCH, 2004)
- [51] C. K. Law, Interaction between a moving mirror and radiation pressure: A Hamiltonian formulation, *Phys. Rev. A* **51**, 2537 (1995)
- [52] M. Tsang and C. M. Caves, Coherent quantum-noise cancellation for optomechanical sensors, *Phys. Rev. Lett.* **105**, 123601 (2010)
- [53] Y. D. Wang and A. A. Clerk, Using dark modes for high-fidelity optomechanical quantum state transfer, *New J. Phys.* **14**, 105010 (2012)
- [54] Y. D. Wang and A. A. Clerk, Using interference for high fidelity quantum state transfer in optomechanics, *Phys. Rev. Lett.* **108**, 153603 (2012)
- [55] C. Dong, V. Fiore, M. C. Kuzyk, and H. Wang, Optomechanical dark mode, *Science* **338**, 1609 (2012)
- [56] Y. Chen, Macroscopic quantum mechanics: Theory and experimental concepts of optomechanics, *J. Phys. B: At. Mol. Opt. Phys.* **46**, 104001 (2013)
- [57] H. Miao, *Exploring Macroscopic Quantum Mechanics in Optomechanical Devices* (Springer, Berlin, 2012)
- [58] L. M. Duan, J. I. Cirac, and P. Zoller, Three-dimensional theory for interaction between atomic ensembles and free-space light, *Phys. Rev. A* **66**, 023818 (2002)
- [59] D. N. Matsukevich, T. Chaneliere, S. D. Jenkins, S. Y. Lan, T. A. B. Kennedy, and A. Kuzmich, Deterministic single photons via conditional quantum evolution, *Phys. Rev. Lett.* **97**, 013601 (2006)
- [60] A. S. Parkins, E. Solano, and J. I. Cirac, Unconditional two-mode squeezing of separated atomic ensembles, *Phys. Rev. Lett.* **96**, 053602 (2006)
- [61] A. V. Gorshkov, A. Andre, M. D. Lukin, and A. S. Sorensen, Photon storage in Lambda-type optically dense atomic media, I. Cavity model, *Phys. Rev. A* **76**, 033804 (2007)
- [62] K. Hammerer, A. S. Sorensen, and E. S. Polzik, Quantum interface between light and atomic ensembles, *Rev. Mod. Phys.* **82**, 1041 (2010)
- [63] S. L. Braunstein and P. van Loock, Quantum information with continuous variables, *Rev. Mod. Phys.* **77**, 513 (2005)
- [64] A. Furusawa and P. van Loock, *Quantum Teleportation and Entanglement: A Hybrid Approach to Optical Quantum Information Processing* (Berlin: Wiley-VCH, 2011)
- [65] A. Ferraro, S. Olivares, and M. G. A. Paris, Gaussian states in continuous variable quantum information, arXiv:quant-ph/0503237 (2005)
- [66] C. Weedbrook, S. Pirandola, R. Garcia-Patron, N. J. Cerf, T. C. Ralph, J. H. Shapiro, and S. Lloyd, Gaussian quantum information, *Rev. Mod. Phys.* **84**, 621 (2012)
- [67] G. J. Milburn, Coherent control of single photon states, *Eur. Phys. J.* **159**, 113/117 (2008)
- [68] F. Khalili, S. Danilishin, H. Miao, H. Muller-Ebhardt, H. Yang, and Y. Chen, Preparing a mechanical oscillator in non-Gaussian quantum states, *Phys. Rev. Lett.* **105**, 070403 (2010)
- [69] N. Yamamoto and M. R. James, Zero-dynamics principle for perfect quantum memory in linear networks, *New J. Phys.* **16**, 073032 (2014)
- [70] J. K. Stockton, J. M. Geremia, A. C. Doherty, and H. Mabuchi, Robust quantum parameter estimation: Coherent magnetometry with feedback, *Phys. Rev. A* **69**, 032109 (2004)
- [71] L. Bouten, J. K. Stockton, G. Sarma, and H. Mabuchi, Scattering of polarized laser light by an atomic gas in free space: A quantum stochastic differential equation approach *Phys. Rev. A* **75**, 052111 (2007)
- [72] M. Tsang and C. M. Caves, Evading quantum mechanics: Engineering a classical subsystem within a quantum environment, *Phys. Rev. X* **2**, 031016 (2012)
- [73] J. S. Prauzner-Bechcicki, Two-mode squeezed vacuum state coupled to the common thermal reservoir, *J. Phys. A: Math. Gen.* **37**, 173 (2004)
- [74] G. Manzano, F. Galve, and R. Zambrini, Avoiding dissipation in a system of three quantum harmonic oscillators, *Phys. Rev. A* **87**, 032114 (2013)
- [75] N. Yamamoto, Decoherence-free linear quantum subsystems, *IEEE Trans. Automat. Contr.* **59**-7, 1845/1857 (2014)
- [76] M. H. Wimmer, D. Steinmeyer, K. Hammerer, and M. Heurs, Coherent cancellation of backaction noise in optomechanical force measurements, *Phys. Rev. A* **89**, 053836 (2014)
- [77] H. M. Wiseman and G. J. Milburn, Quantum theory of field-quadrature measurements, *Phys. Rev. A* **47**, 642 (1993)
- [78] A. Isidori, *Nonlinear Control Systems*, 3rd ed. (Springer, 1995)
- [79] H. Nijmeijer and A. van der Schaft, *Nonlinear Dynamical Control Systems*, 3rd ed. (Springer, 1996)
- [80] G. I. Harris, D. L. McAuslan, T. M. Stace, A. C. Doherty, and W. P. Bowen, Minimum requirements for feedback enhanced force sensing, *Phys. Rev. Lett.* **111**, 103603 (2013)
- [81] H. M. Wiseman, Quantum theory of continuous feedback, *Phys. Rev. A* **49**, 2133 (1994)
- [82] Usually the controllable and uncontrollable subspaces are defined by $\text{Range}(\mathcal{C}_u)$ and $\text{Range}(\mathcal{C}_u)^c$, respectively. But in the quantum case a variable of interest is an infinite-dimensional operator and does not live in either of these subspaces; rather it is always of the form $v^\top \hat{x}$ and thus can be well characterized by the dual vector $v \in \mathbb{R}^{2n}$. This is the reason why we define the controllable and uncontrollable subspaces in the dual space as $\text{Ker}(\mathcal{C}_u^\top)^c$ and $\text{Ker}(\mathcal{C}_u^\top)$, respectively.